

**CZECH UNIVERSITY OF LIFE SCIENCES PRAGUE**

Faculty of Agrobiological Sciences, Food, and Natural Resources

Department of Water Resources



**Czech University  
of Life Sciences Prague**

**Influence of Urban Development on Meteorological  
Elements Influencing the Microclimate in Prague-Suchdol,  
Czech Republic**

**DIPLOMA THESIS**

Author: BSc. Bunthorn Thet  
Natural Resources and Environment

Supervisor: Ing. Markéta Miháliková, Ph.D.

Consultant: Ing. Věra Kožnarová, CSc.

*Declaration*

I hereby declare the thesis titled "-Influence of Urban Development on Meteorological Elements Influencing the Microclimate in Prague-Suchdol, Czech Republic" has been composed by myself and the work has not summited by any others degree or professional qualification. I confirm that the work that summited is my own and all scientific literature and sources that I quoted are cited and acknowledged in the references. Being an author, I certify that I did not copy from the third person.

In Prague, April 26, 2021

Signature: .....

## *Acknowledgements*

I would like to express my sincere gratitude to my supervisor Ing. Markéta Miháliková, Ph.D., for her valuable guidance, continuous support, and time throughout my research. You provided me with the tools that I needed to choose the right direction and successfully complete my thesis. Moreover, I would also to extend my gratitude to my senior and friends who always stay by my side for motivating and helping me for data analyzing and consultation. I really appreciate and have a great honor to work with them.

I would also like to thank my thesis consultant Ing. Věra Kožnarová, CSc, who provided the idea of the thesis and significantly contributed to the quality of the thesis by her valuable comments, time, and effort.

I would like to deeply thank the Czech government that provided scholarships for Cambodian students to study in the Czech Republic. This scholarship truly helped many Cambodian students to strengthen their abilities, knowledge, and perceptions. To me, this scholarship is like a priceless thing that I obtained

In additional, I would like to thank my family and friends who always supported, motivated, encouraged and taught me when I needed them throughout the whole master's degree. Their love and kindness are bringing me to achieve my goal.

# **Influence of Urban Development on Meteorological Elements Influencing the Microclimate in Prague-Suchdol, Czech Republic**

## **Summary**

Urban development usually involves the replacement of natural features with physical infrastructure and there is a perception that urbanization influences microclimate. In order to understand the extent to which such development affects microclimate, there is need to quantify meteorological elements such as air temperature, air humidity, air pressure, daily precipitation totals, global radiation, wind speed and wind direction for a specified period of time. The objectives of the study were to investigate the microclimate patterns between 2013 and 2020 within the urban and rural areas of CZU campus, represented by Meteostation of the Czech University of Life Sciences Prague, operated by the Department of Agroecology and Crop Production (further denoted as CZU station), and Experimental Terrain Station of Soil Moisture Dynamics, operated by the Department of Water Resources (further denoted as DWR station), respectively. Data of the above-mentioned meteorological variables were evaluated, specifically the month June, in which the biggest differences were expected. Data were collected mostly in 10 or 15 min interval and then compared and statistically evaluated on hourly or daily basis. The result showed that, for most variables the differences were not significant, when combined the effect of year and station, but separately there were differences. Thus, air humidity was slightly higher at CZU, temperature was slightly higher at DWR, daily precipitation was slightly higher at CZU. Therefore, the climate record showed that the air temperature in hourly average in 2019 was much higher than other years (22.18 °C, SD 5.16 °C from CZU and 22.60 °C, with SD 5.19 °C from DWR), it was above normal average because of heat wave event. Daily precipitation totals in 2013 illustrated the highest amount 5.78 mm/day, SD 14.51 mm/day from CZU and 4.76 mm/day, SD 9.31 mm/day from DWR, due to heavy rain and flooding event in that year. For these reasons, both stations CZU and DWR indicated that air humidity was lower in 2019 about 56.36 %, SD 19.91 % and 54.71 %, SD 20.65% and higher in 2013 71.07 %, SD 17.07 % and 69.34%, SD 17.72%. For overall, the result showed that the comparison between CZU and DWR were statistically significant ( $P\_value < 0.05$ ). Urban development has a great impact on wind speed and wind direction variable due to higher roughness of the area.

**Keywords:** *microclimate, urban heat island, weather variables, meteorological station*

## Contents

Summary .....	iii
List of Figures .....	vi
List of Tables .....	viii
1. Introduction.....	1
2. Scientific hypothesis and objectives .....	2
2.1 Hypothesis.....	2
2.2 Objectives.....	2
3. Literature review.....	3
3.1 Condition of rural meteorological station .....	3
3.2 Weather variable characteristic in urban area .....	3
3.3 Meteorological variables obtained at meteorological stations .....	4
3.3.1 Air humidity.....	4
3.3.2 Estimation of relative humidity from temperature .....	4
3.3.3 Air pressure.....	5
3.3.4 Air temperature .....	8
3.3.5 Daily precipitation totals.....	9
3.3.6 Global radiation .....	11
3.3.7 Temperature extreme .....	13
3.3.8 Wind speed and direction .....	14
4. Materials and methods .....	16
4.1 Location .....	16
4.2 Urban meteorological station (CZU) .....	16
4.3 Rural meteorological station (DWR).....	17
4.4 Observation of meteorological variables .....	18
4.4.1 Measurement of air humidity.....	19
4.4.2 Measurement of air pressure.....	19
4.4.3 Measurement of air temperature .....	19
4.4.4 Daily precipitation totals.....	19

4.4.5	Measurement of wind speed and direction .....	21
4.4.6	Measurement of global radiation .....	21
4.5	Statistical analysis .....	24
5	Results.....	25
5.4	Air humidity .....	25
5.5	Air pressure .....	29
5.6	Air temperature .....	30
5.7	Temperature extreme .....	35
5.8	Daily precipitation totals .....	37
5.9	Global radiation.....	40
5.10	Wind speed and direction.....	43
6	Discussion.....	50
6.4	Effect of air humidity .....	50
6.5	Effect of air temperature, and temperature extreme.....	50
6.6	Effect of daily precipitation totals.....	51
6.7	The effect of global radiation based on direction sunlight.....	52
6.8	Effect of wind speed and direction according to urban development.....	53
6.9	Effect of weather viable between urban and open field meteorological station .....	54
7	Conclusion .....	55
	Bibliography .....	56
	Appendices.....	65

## List of Figure

Figure 1 Boreal winter sea level pressure anomalies (Dunn, 2019) .....	6
Figure 2 the mercury barometer (Robert, 2008) .....	7
Figure 3 heat wave event in the last week of July 2019 in Western Europe (World weather Distribute, 2019) .....	9
Figure 4 Schematic diagram illustrating the interaction of solar radiation with atmospheric particles (aerosols, clouds, and air molecules) (Kanniah et al. 2012) .....	12
Figure 5 Time series of temperature extreme from 1956 - 2020, China (Wang et al., 2012)...	13
Figure 6 . Schematic overview of the model between and urban area and the character of wind speed (Droste et al. 2018) .....	15
Figure 7 Meteorological stations located in CZU campus ( <a href="https://en.mapy.cz/">https://en.mapy.cz/</a> ). .....	16
Figure 8 CZU meteorological station representing the urban conditions ( <a href="https://en.mapy.cz/">https://en.mapy.cz/</a> ). .....	17
Figure 9 DWR Meteorological station ( <a href="https://en.mapy.cz/">https://en.mapy.cz/</a> ).....	18
Figure 10 Rain gauge precipitation record Model SR03 .....	20
Figure 11 MR3H tipping-bucket rain gauge (TBR-MR3H).....	20
Figure 12 Switching of ANEMOMETER (A100R) .....	21
Figure 13 Pyranometer (LP02 Hukseflux) of solar radiation record .....	22
Figure 14 Temporal variation of air humidity in hourly average .....	25
Figure 15 Scatter plot of air humidity hourly average from CZU and DWR meteorological station.....	26
Figure 16 Air humidity diurnal difference between CZU and DWR meteorological station...28	
Figure 17 Scatter plot Relationship of air humidity diurnal difference .....	28
Figure 18 Temporal air pressure hourly average from 2013-2020 .....	29
Figure 19 Temporal variation of air temperature in hourly average at 2 m.....	31
Figure 20 Scatter plot illustrating the relationship of air temperature hourly average .....	32
Figure 21 Time series diurnal difference of air temperature from two different weather stations .....	34
Figure 22 Scatter plot illustrating the relationship diurnal difference of air temperature .....	34
Figure 23 Historical of temperature extreme in daily average at 2 m from 2013-2020 .....	35
Figure 24 Scatter plot illustrating the relationship of temperature extreme daily average .....	36
Figure 25 Average daily precipitation totals from two different weather station.....	38
Figure 26 Scatter plot relationship of daily precipitation totals.....	39

Figure 27 Historical of solar radiation hourly average from (2013-2020) .....	40
Figure 28 The comparison of global radiation between morning and afternoon.....	41
Figure 29 Demonstration of the differences between morning and afternoon values of global radiation in both stations.....	41
Figure 30 Temporal of global radiation in hourly average between CZU and DWR meteorological station.....	42
Figure 31 Wind and direction in hourly average of CZU meteorological station during the statistical period of (2014-2020) and colored according to different wind speed .....	44
Figure 32 wind rose of Wind speed and direction in hourly average measured at DWR meteorological station and colored according to different wind speed .....	45
Figure 33 Historical climate record of wind speed hourly average from two different station	46
Figure 34 Correlation of wind speed hourly average between CZU and DWR meteorological station.....	47
Figure 35 shows the variation of the hourly average wind direction at 2 m above the ground surface.....	48



## List of Tables

Table 1 General of statistic of daily precipitation indices (Wang et al. 2019) .....	11
Table 2 Hourly average of air humidity observed from CZU and DWR station according to ANOVA in Statistica ( $P < 0.05$ ). .....	26
Table 3 Overall statistic of air humidity hourly average. ....	27
Table 4 Summary of statistical information of air pressure in hourly average.....	30
Table 5 ANOVA of air temperature in hourly average .....	31
Table 6 Descriptive statistics of air temperature in hourly average between CZU and DWR station.....	33
Table 7 ANOVA of temperature extreme daily average summary .....	36
Table 8 Summary of statistic of temperature extreme in daily average .....	37
Table 9 ANOVA of daily precipitation totals.....	38
Table 10 Summary statistic of daily precipitation .....	39
Table 11 ANOVA of global radiation in hourly average summary.....	42
Table 12 Summary of statistic of global radiation hourly average.....	43
Table 13 ANOVA comparison of wind speed hourly average .....	46
Table 14 Summary of statistic of wind speed hourly average .....	47
Table 15 ANOVA of wind direction in hourly average .....	48
Table 16 Overall results of ANOVA for each variable .....	49

# 1. Introduction

The improvement of urban area is particularly increasing due to high intensity of population and infrastructure development. However, the impact of urbanization created the urban heat islands (UHIs) in which exacerbate the risk of heat-related mortality associated with global climate change. The investigate the morphology of microclimate between urban and rural area will contribute to the mosaic of different environmental data about the university campus and experimental fields in close vicinity of the DWR station. Therefore, the two meteorological stations are located for several years close to each other, but until now there was no comparison between them carried out. The direct implication of these evaluation might be bringing out the characteristic of climate between rural and urban area. The historical weather record has always been of great significance how the urban climate has been changed. For the data from meteorological station are of the central importance to maximize characteristic of climate through optimized control. However, microclimate plays an important role for agricultural activity to extend its size to meet the population growth, natural ecosystems development and prevention, and habitat destruction in this case use for predicting the climate characteristic for field research (Prado et al. 2021). Furthermore, weather is usually described in terms of a series of measurements and observations that include temperature, wind, humidity, cloud cover and precipitation. The values of meteorological variables vary in time and due to climate change and error accuracy of the station instrument. It is shown that reference years obtained from longer periods are not representative of the most recent years, which present higher dry-bulb air temperatures due to a short-term climate change effect of the historical weather record (Libralato et al. 2020). The increased interest in environmental issue and variability has created a demand for observing about past meteorological data (Rodrigo, 2012) The characteristics of the microclimate between two meteorological stations are about to understand the changing relative between the open space and urban area and needed to be better understood and to improve e.g., the quality of human well-being or reliability of models for crop growth and to formulate management recommendations (Robetez, 2018). Particularly, weather variable had been measuring with different instrument due height, depth, size, and kind of difference type of instruments are to be used for recording the meteorological variables with high precision (Hubbard el al. 2015). Recently, automatic meteorological instruments are becoming increasingly important for measuring the meteorological parameters and have provided the weather record for local people.

## **2. Scientific hypothesis and objectives**

### **2.1 Hypothesis**

Data from the two meteorological stations will show different microclimate resulting from modification of land surfaces. Urban area will be significantly warmer than rural area with greater diurnal temperature variation.

### **2.2 Objectives**

The main objective of the thesis is to compare selected meteorological data from several years from two meteorological stations, both located in Prague-Suchdol but in different environments in terms of urban development representing the rural and urban microclimate, and to evaluate the effect of urbanization on the local microclimate.

### **3. Literature review**

#### **3.1 Condition of rural meteorological station**

An important of weather collection consists in the possibility of utilizing completely automatic stations installed at isolated locations, such as mountain peaks, islands, etc., whereby information on the meteorological factors of interest is automatically transmitted at preestablished intervals (Diamond et al., 1940). Measurements typically made at such stations include air temperature, relative humidity, wind speed and direction, precipitation, and solar radiation (Giannopoulou et al. 2010) weather variable are slightly difference between urban and rural area based on convective loss and gain. So, the measurement weather in rural is significantly information for agricultural purpose and field research. Hubbard et al. (2005) had address that the meteorological station is generally located at agricultural research field, branch campuses, or other locations within a region. These networks are the result of the development of relatively low-cost automated weather stations that measure and record meteorological variables. Recently, the use of electronic process and miniaturization of circuits-sensor have been invented, it's possible to collect the number of weather variable more precise and faster. The results embellish the context in which environmental–physical activity relationships should be interpreted and provide important information for researchers applying the observation method in open-air settings (Suminski et al. 2008).

#### **3.2 Weather variable characteristic in urban area**

Urban area is particularly where human settlement with higher population and high standard of infrastructure mainly in the coming decade are expected to be expanded. Changes in the near-surface climate of cities are involved significant for human health and energy use, as the result they have produced extreme climate events in those area. Moreover, urban development typically modifies surface energy and radiation budgets by changing the vegetable cover, cause air temperature in surface and creating urban heat islands (Wang, 2017). Since the application of the reform and opening policy in Czech University of Life Sciences in the late 2000s, the meteorological stations located inside tall building due to urban expansion and extending the institution building. Urban expansion around meteorological station have influenced observations of meteorological variables especially air temperature and urban heat island mainly effect does occur due to urban expansion, with a higher intensity in winter than in other seasons (Shao, 2011). However, meteorologically are often hotter than surrounding vegetable or undeveloped area and rapid urbanization has transformed cities into a collection of buildings

with variable heights that generate strong wind turbulence and low average wind speeds (Wang, 2017 & Byrne et al. 2018). These types of results can provide valuable information for urban planners and decision-makers for evolving strategies against the adverse effects of urban climate and climate change to create livable settlements (Unger, 2020). Therefore, the collected meteorological data can also be used for different applications in urban meteorological modelling (Matzarakis, 2008).

### **3.3 Meteorological variables obtained at meteorological stations**

#### **3.3.1 Air humidity**

The term atmospheric humidity refers to the water vapor content of the atmosphere. However, water vapor entering atmosphere by evaporation, primarily from the surface water such as ocean, river, lake, and all surface water. As the result, water vapor carries out over the earth's surface by presenting of the wind. The main principle of increasing the water vapor in the air is temperature. Moreover, Relative humidity (RH) in air is very important variable used in different industries such as chemical, food, agriculture, and climate. Conventionally, mechanical hygrometer, chilled mirror hygrometer, and electronic sensors are used for measuring of relative humidity (Lin et al. 2020). In such region the relative humidity is very low in the early afternoon, when the temperature is maximum, while at night the air may be almost saturated. Air humidity are particularly important because of their relevance to the changes of state of water in the atmosphere. There are several instruments for measuring air humidity: A simple psychrometer is a set of dry bulb and wet bulb thermometers of identical form and size exposed in a Stevenson's Screen. The dew point temperature and relative humidity are then estimated from the hygrometric tables.

#### **3.3.2 Estimation of relative humidity from temperature**

Humidity measurements at the Earth's surface are required for meteorological analysis and forecasting, for climate studies, and for many special applications in hydrology, agriculture, aeronautical services, and environmental studies, in general. Relative humidity is most conveniently estimated using Dry Bulb and Wet Bulb temperatures. Kanniah et al. (2012) August's modification of Regnault's formula (temperature in °C instead of °F) for calculation of vapor pressure and thus the hygrometric. The equation is given as follows:

For temperatures of wet bulb below 0 °C:

$$x = f - \frac{0.480 (T - T')}{671 - T'} \times P$$

For temperatures of wet bulb above 0 °C:

$$x = f' - \frac{0.480 (T - T')}{610 - T'} \times P$$

Where:

X Pressure of vapor present in the air

$f'$  Saturation vapor pressure at temperature of the Wet Bulb

T Temperature of the Dry Bulb in °C

T' Temperature of the Wet Bulb in °C

P Pressure of air.

### 3.3.3 Air pressure

The atmospheric pressure is the weight exerted by the overhead atmosphere on a unit area of surface in each horizontal cross-section and mainly air flow from higher pressure to lower pressure zone. However, the flow is not in the direction of the greatest pressure gradient, at right angles to the lines of equal pressure (isobar) but is deflected by a phenomenon known as the Coriolis force, resulting from the rotation of the earth (WMO, 2010). In general, there are belts and center over hemisphere of the earth's surface of low and high atmosphere. During the wintertime, both are continuous round the earth brings the pressure over the continents is higher than over the ocean. On the other hand, in summer, low- pressure center (depressions) develops over the continents, interrupting the continuity of the belts (Givoni, 1969). Atmospheric pressure drops as altitude increases. As the pressure decreases, the amount of oxygen available to breathe also decreases. At very high altitudes, atmospheric pressure and available oxygen get so low that people can become sick and even die. Atmospheric pressure is very significant due to variation in pressure within the atmosphere system creates our atmospheric circulation and influences our weather and climate (Robert, 2008).

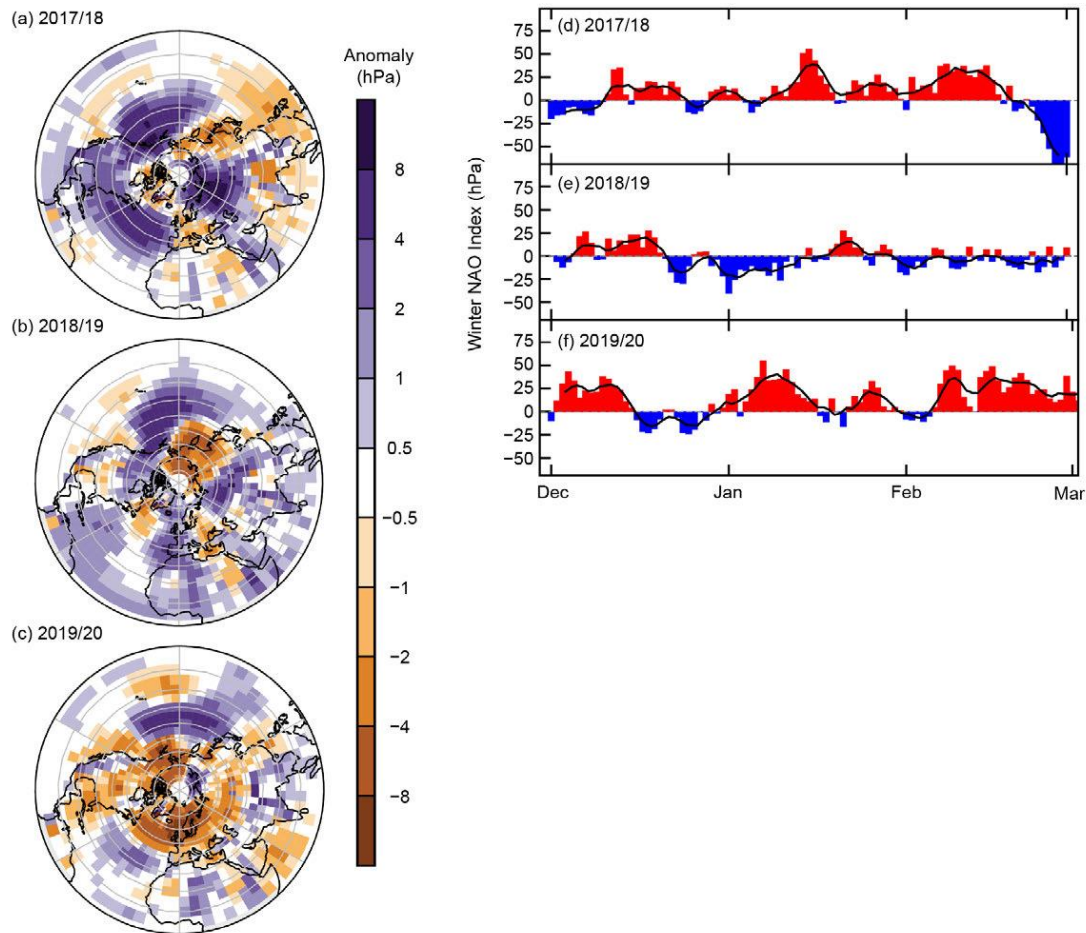


*Figure 1 Boreal winter sea level pressure anomalies (Dunn, 2019)*

Barometer is commonly used for measurement atmospheric pressure. The principle of the barometer, a column of mercury in a glass tube rises or falls as the weight of the atmosphere changes. Meteorologists describe the atmospheric pressure by how high the mercury rises (Rutledge, 2011). Air pressure can simply be measured with a barometer by measuring how the level of a liquid changes due to different weather conditions. When we don't have columns of liquid many feet tall, it is best to use a column of mercury, a dense liquid. The aneroid barometer measures air pressure without the use of liquid by using a partially evacuated chamber. This bellows-like chamber responds to air pressure so it can be used to measure atmospheric pressure.

In 1643, a student of Galileo name Evangelista Torricelli performed an experiment about the basis for the invention of the mercury barometer, an instrument that measures atmospheric pressure. Torricelli took a tube filled with mercury and inverted it in an open pan of mercury. The mercury inside the tube fell until it was at a height of about 76 centimeters (Robert, 2008)



*Figure 2 the mercury barometer (Robert, 2008)*

In meteorology, the unit of atmospheric pressure is in hectopascals (hPa). Generally, 1 hPa is equal to 100 Pa, the pascal being the basic SI (System of International Unit). 1 Pa is equal to 1 Newton per square meter (N/m<sup>2</sup>). And 1 hPa is equal to 1mb that was used formerly. The principle of mercury barometer is to measure atmospheric pressure from precise measurement of the height.

The correction value for temperature  $Ct$  is expressed as follows:

$$Ct = -H \frac{(\mu - \gamma)t}{1 + \mu t}$$

Where:

$H$  is the barometric reading after the correction for index error (hPa)

$t$  is the temperature indicated by the attached thermometer ( $^{\circ}\text{C}$ )

$\mu$  is the volume expansion coefficient of mercury.

$\lambda$  is the linear expansion coefficient of the tube.



### 3.3.4 Air temperature

Air temperatures determine by the rate of heating and cooling of the surface of the earth surface. In the free atmosphere, air temperature decreases with altitude up to the stratosphere. Global warming has been increasing and causing various issue both human and environment. Extensive evidence has been documented to show that Earth's surface air temperature has risen by  $0.6 \pm 0.2^{\circ}\text{C}$  since the end of the 19th century, with warming in the Northern Hemisphere more apparent and up to or greater than  $1^{\circ}\text{C}$  (Shao, 2011). The average temperature of air is higher in summer and lower in winter over land than over the sea. Air temperature is a key variable in affecting biotic communities' energy and water consumption and human comfort and health. Temperature is a greater interest in agricultural applications because it is a driving variable that determines the rate of growth and development of an organism, and thus determines what species can grow in a region (Hubbard, 2015). Results can enhance our theoretical understanding of the spatial heterogeneity of the urban thermal environment and have practical indication on excessive urban heat mitigation and adaptation in an increasingly warming global climate (Cao, 2021). However, the increase in the use of construction materials such as extending the space of the building with the amount of the population in cities and caused the rising temperature in city and creating the effect known as urban heat island. Because, in urban area were primarily covered by vegetation were carried out the free air movement are replaced by infrastructures such as streets, houses and buildings. In this regard, recording the historical air temperature mainly is to mitigate the effects of urban heat islands (Carpio, 2020). Unanimously, the rise on air temperature is an undeniable fact confirmed at almost all places in the world and the pattern of air temperature is depending on the variable in surface temperature (Bartoszek, 2021 & Givoni, 1969). The global warming is reflected into the land and ocean surface as the result of the lake and permafrost temperatures have changed from low to high, glaciers have continued to lose mass, becoming thinner for the 32nd consecutive year, with the majority also becoming shorter during 2019. There were fewer cool extremes and more warm extremes on land; regions including Europe, Japan, Pakistan, and India all experienced heat waves (Bluuden et al. 2020).

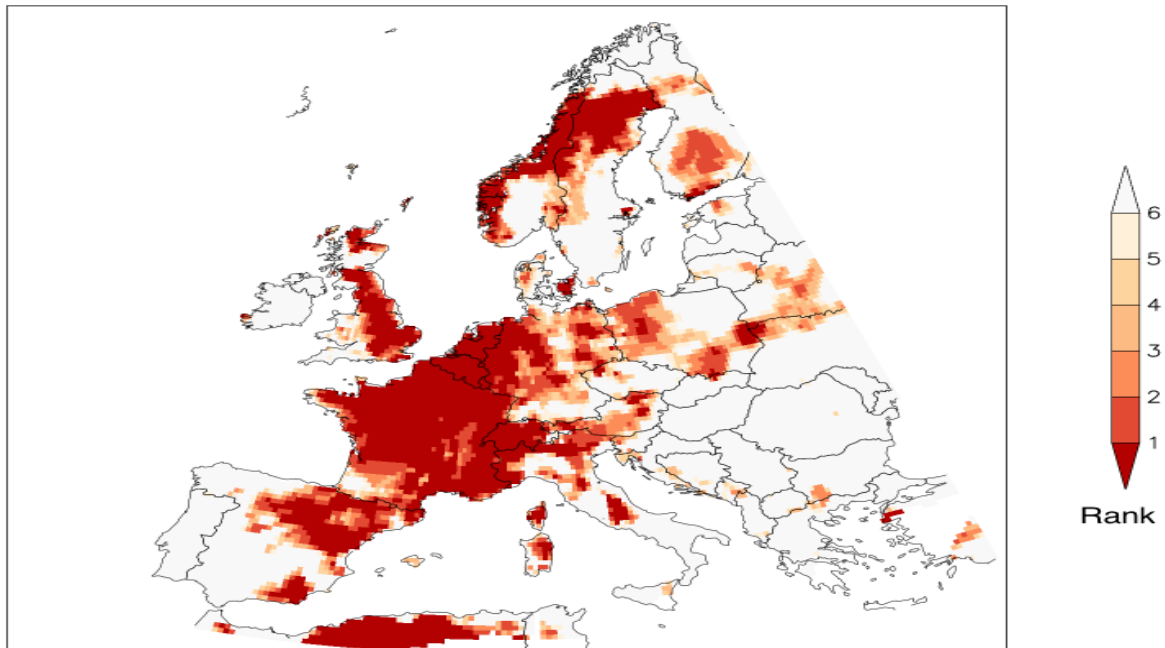


*Figure 3 heat wave event in the last week of July 2019 in Western Europe (World weather Distribute, 2019)*

Based on <http://www.meteo-technology.com/temperature.htm> the most usual temperature measurement is that of air temperature. The measurement is easily disturbed particularly by solar radiation. Thermometer instrument is used for Air temperature measurement since the early 1600s until today. The reference concept of thermometer has based on the degree of heat and cold by Greek physician Galen (Middleton, 1969). Thermometer is the result of a long trial and error process. It began with a physiological description of temperature and evolved to the present state. The different stages in its development reflect the state of science at the time as well as the ingenuity of scientists to realize and overcome the shortcomings of science during each stage (Wisniak, 2000). As consequence, the mean value that conventional conversion formulae need to be applied to express them in degrees Celsius and the comparison between simultaneous temperature data from two different sources allowed associate up to 1°C as error margin provoked using different instruments. (Rodrigo, 2012).

### **3.3.5 Daily precipitation totals**

Precipitation is one of the most significant meteorological variables for agriculture and it had known as all forms of moisture that falls from the atmosphere to the ground such as rain, drizzle, snow, ice, hail, diamond dust, snow grains, snow pellets, ice pellets, rime, glaze, frost and dew, and any deposit from fog. However, the drought event occurs when it has no precipitation or less than the evaporation in contract excessing of precipitation results in flooding issue over the specific area (Selase et al. 2015 & Hubbard, 2005). The precipitation is

used interchangeably with the amount of rainfall; however, it refers all forms of condensation of water vapour both solid and liquid products falling from clouds or deposited onto the ground (Mekonnen et al. 2015). Precipitation has been known as the important element of water cycle in the Earth System, which is closely related to ecological, hydrological, and meteorological processes. Its spatial and temporal variations generally influence vegetation distribution, soil moisture and surface runoff (Shi et al. 2015). However, precipitation occurs when a mass of rising air cools by expansion and reaching its dew point. Then the large-scale condensation occurs, in which tiny droplets of water were formed as clouds composed of innumerable tiny water droplets and sometimes ice crystals. Heavier droplets begin to form as the air continues to rise and when they are large enough to fall and withstand the evaporative loss during the descent (Givoni, 1969). Air masses which are made to rise for different reasons produce three main types of precipitation: convection, orographic and convergent. Extreme precipitation events have caused economic and social losses throughout history around the world. Moreover, numerous studies have demonstrated their intensification in response to the warming climate. Precipitation data is also useful for exploring the risks related to extreme precipitation events (Serrano-Notivol et al. 2018). The daily precipitation totals are not as common as monthly or annual-scale ones, it is used for daily records for predicting the amount of rainfall on the ground (Harris et al. 2014). However, daily rainfall heterogeneity and regional geomorphology can be partly interpreted; the precipitation concentrations explain the cause of why some regions are vulnerable to be influenced by high intensity precipitation events, spatial distribution of different intensities, however, few researchers pay attention to the statistical structure of daily precipitation in recent years. (Wang et al. 2019)

Meanwhile, the amount of rainfall recorded at a place is measured by an instrument called a rain gauge. A rain gauge is a copper cylinder with a collection jar inside and a funnel on top. The gauge is placed into the ground leaving only 30cm of the top above the ground level to prevent splashing water from entering it. Rain falls through the funnel on top of the copper cylinder and is collected into the jar. The water is collected after 24 hours, and then poured into a measuring cylinder for measurement to be taken (Selase, 2015). Rain gauges are classified into recording and non-recording types. According to Mekonnen et al. (2015) both in the field and the laboratory precipitation records have highlighted the need to properly calibrate and correct TBRs for rainfall measurements to properly calibrate and correct TBRs for rainfall measurements.

Table 1 General of statistic of daily precipitation indices (Wang et al. 2019)

Parameter		Min	Max	Mean	Std.	CV
P		228.88	818.84	515.10	110.17	21.39
RD		3.02	6.14	5.04	0.75	14.86
CI		0.69	0.76	0.72	0.01	2.08
Contribution of rainy days (%)	Low	23.30	33.57	28.59	1.51	5.27
	Moderate	25.78	36.53	31.07	1.60	5.15
	High	19.47	21.08	20.21	0.31	1.56
	Very high	19.70	20.39	20.13	0.11	0.57
	Extreme	9.82	10.21	10.04	0.07	0.66
Contribution of precipitation amounts (%)	Low	0.95	2.01	1.33	0.20	15.34
	Moderate	5.68	9.81	8.14	0.73	9.01
	High	15.34	20.26	18.21	1.00	5.49
	Very high	68.70	77.02	72.32	1.65	2.28
	Extreme	48.65	57.09	52.01	1.79	3.45

Based on Wang et al. 2019 have found that the amount of precipitation and relatively were less rainy days, more concern should be paid to the two categories due to the high contribution, which may trigger negative influence on the environment.

### 3.3.6 Global radiation

Solar Radiation is an electromagnetic radiation emitted from the Sun and can be transferred into useful forms of energy, such as heat, and electricity based on varieties of technology (Givoni, 1969). The different wavelengths called solar spectrum is broadly divided into the Ultraviolet waves shorter than 0.4 micrometer ( $\mu\text{m}$ ) (U.V), the visible waves between 0.4 to 0.76 micrometer ( $\mu\text{m}$ ) and the waves longer than 0.76 micrometer ( $\mu\text{m}$ ) known as infra-red. However, radiation is the transfer of energy via electromagnetic waves that travel at the speed of light. The speed of light in a vacuum is about  $3 \times 10^8$  m/s. Moreover, the duration of transferring the light from the Sun to reach the Earth is 8 minutes and 20 seconds. Additionally, the amount of solar energy reaching the earth surface depends on the sky clearance with respect to cloud, and the purity of the air with respect to dust, carbon dioxide and water vapor: those factors which must be evaluated instead of calculated exactly. One that point was reached,

when small particles and gas molecules diffuse part of the incoming solar radiation in random directions without any alteration to the  $\lambda$  of the electromagnetic energy this process called scattering. In this regard, Absorption is defined as a second process in which solar radiation is retained by a substance and converted into heat. However, Reflection is known as the third process in atmosphere where sunlight is redirect by  $180^\circ$  after it affected an atmospheric particle. In fact, the duration of the sunlight, however, increases in summer cause the duration of the day is longer and is reduced in winter that is the daytime is shorter, with increasing latitude. Consequently, the variation in the solar radiation resulted in a yield gap and different cultivars behaved differently. The aboveground and underground growth responses to different level of global radiation indicated the difference in yield gap (Yang, 2021). Kanniah et al. (2012) Clouds and atmospheric aerosols are two main factors variables that determine the possibility of light reaching the surface either the rate of photosynthesis or carbon accumulation in plants. However, Changes in solar radiation because of clouds and aerosols thus can modify the carbon balance of terrestrial ecosystems.

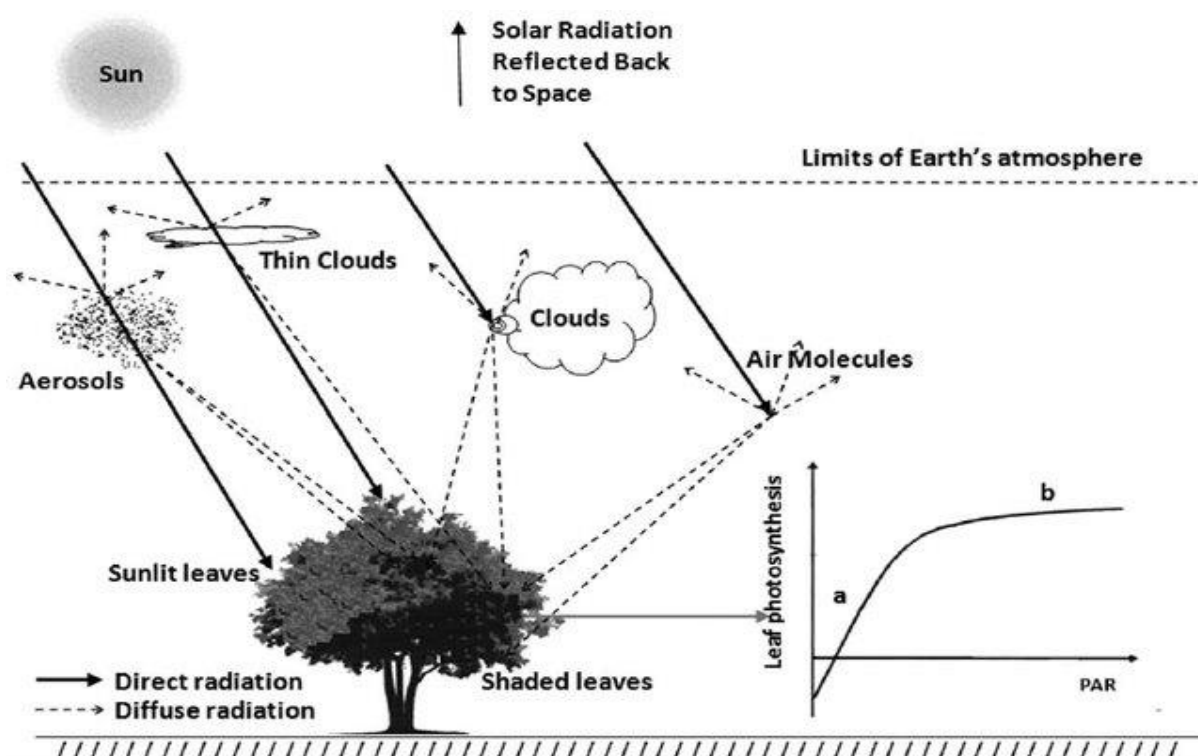


Figure 4 Schematic diagram illustrating the interaction of solar radiation with atmospheric particles (aerosols, clouds, and air molecules) (Kanniah et al. 2012)

### 3.3.7 Temperature extreme

The term of temperature extreme indicates the occurrences of cold days, cold nights, warm days, and warm nights with varying intensities. Temperature extremes have been paid great attention and regarded as a main issue of the global and both extreme low and frost days decreased in the past. In this regard, the highest temperatures increased in recent decades, with the increasing trend of the lowest temperature being much greater than that of the highest one. (Wang, 2012). As changes in the risks of temperature extremes are often associated with changes in the temperature probability distribution, further analysis is still needed to improve understanding of the warm extremes over China. Changes in the occurrence probability of warm extremes are generally well explained by the combination of the shifts in location and scale parameters in areas with grown variability (Chen, 2020). The result of negative impact of rising air temperature are higher energy demand for air conditioning, risk of power failure, and an increased rate of sickness and mortality. One of the most common of extreme high air temperature events in July- August 2003 are the heat wave in central-western Europe such as France, Italy, and Britain and in July–August 2010 in central-western Russia (Valeriánová, 2017) Considerable attention has recently been paid to identification of large scale atmospheric conditions leading to extremely high air temperatures in Central Europe, high air temperature events are especially influenced by high pressure situations was blocking over western Russia. There is a close relationship between surface high temperature extremes and the appearance of climatologically high or low values of certain thermo-dynamic variables in specific locations in the free atmosphere. The occurrence of temperature extremes in the CZ is usually connected with a flow of tropical air to Central Europe.

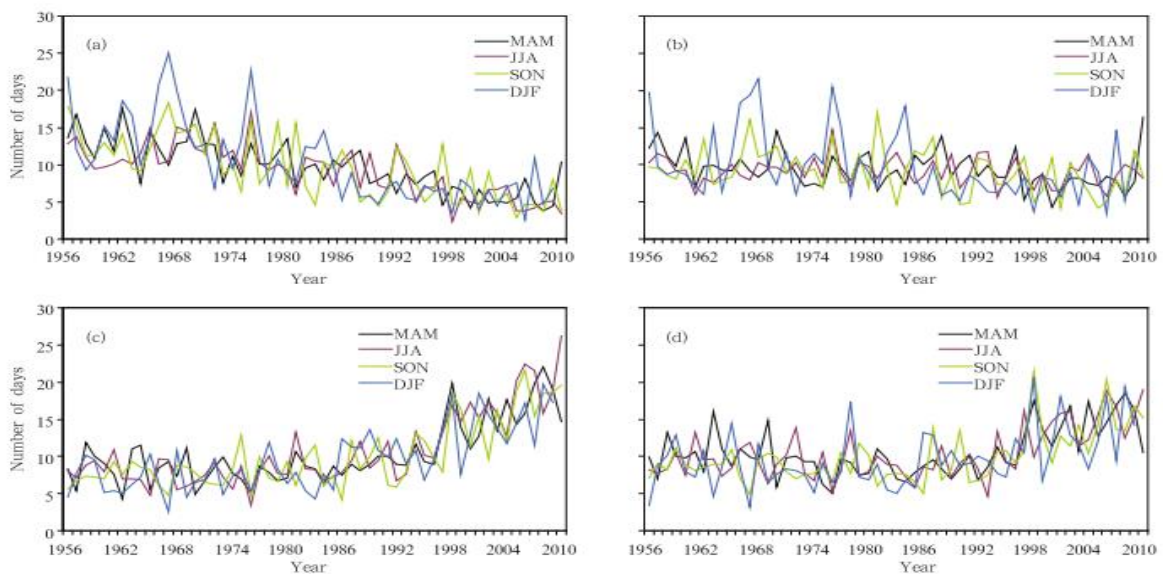


Figure 5 Time series of temperature extreme from 1956 - 2020, China (Wang et al., 2012)

### 3.3.8 Wind speed and direction

Wind results from a horizontal difference in air pressure and since the Sun heats different parts of the Earth differently, causing pressure differences, the Sun is the driving force for most winds. Winds are the air flow as the result from the tendency of air masses that have undergone different amount of heating, and that therefore have developed unequal pressure, to equalize those pressure and the air flow from region of high pressure to low pressure. There are three global belts of winds in each hemisphere are (a) the trade wind (b) the waterlies wind (c) the polar winds (Cann and Colin, 2008). Therefore, the highest of population in the city and urban expansion will increase economic activity as well as more construction as built as the result of taller building in city center and development urban area can be modified air flow and create strong wind will be increasing the air temperature. According to Dutch scientist wind speed was categories as greater than  $5 \text{ m. s}^{-1}$  as strong as greater than  $15 \text{ m. s}^{-1}$  limited risk and dangerous. However, Wind speeds measured by urban weather stations are generally lower than similar data measured in open field meteorological station (Swarno et al. 2020). Wind speed would be slower under the shade, which would limit evaporation of water droplets on leaves. These changes would create microclimate conditions favorable for the development of plant diseases (Kyu, 2015). The measurement of wind speed and direction has always been of great significance in various industries, including meteorology, wind power industry, construction industry, agricultural industry, and transportation. Wind speed is usually measured by anemometers (Bai et al., 2021). The result of wind speed and direction is very useful for the design and construction of buildings with good airflow and strong structures in urban areas and for agriculturalist as well (Swarno et al., 2020). There are mainly three types of anemometer in the market, which are ultrasonic, thermal as well as mechanical anemometers. Anemometers and wind vanes are mounted on masts at the height of 11 m above ground. The data are stored every 10 minutes by data loggers (Campbell Scientific) (Fortuniak, 2006).

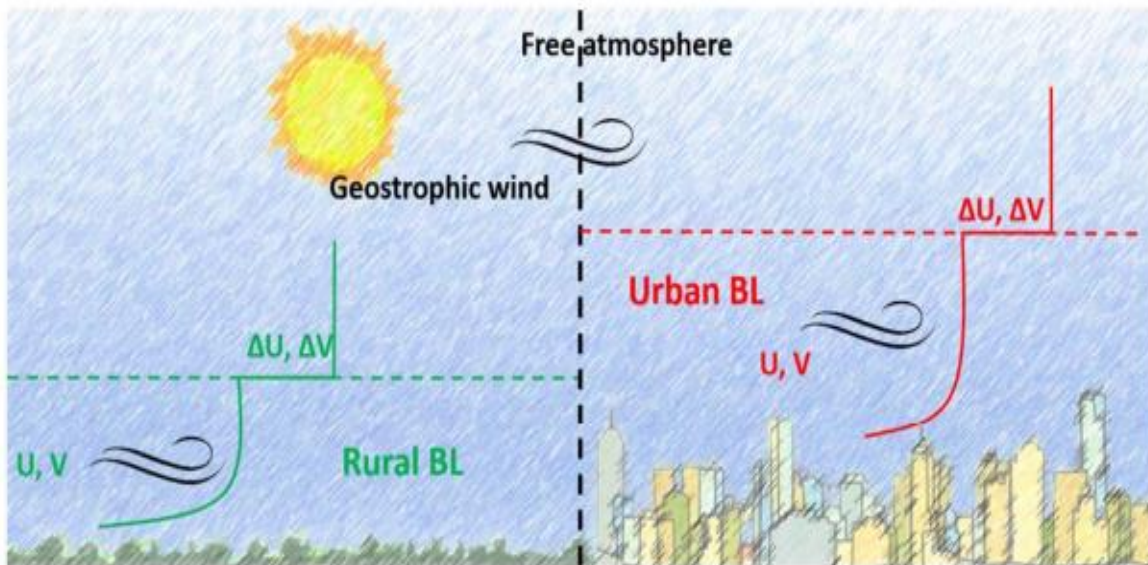


Figure 6 . Schematic overview of the model between and urban area and the character of wind speed (Droste et al. 2018)



## 4. Materials and methods

### 4.1 Location

This study was carried out in the Czech University of Life Sciences Prague campus, a north-western suburb of Prague. Urban microclimate was represented by Meteorostation of the Czech University of Life Sciences Prague, operated by the Department of Agroecology and Crop Production (further denoted as CZU station), while rural or open space microclimate was represented by Experimental Terrain Station of Soil Moisture Dynamics, operated by the Department of Water Resources (further denoted as DWR station), see Figure 7.



Figure 7 Meteorological stations located in CZU campus (<https://en.mapy.cz/>).

Both stations and all measurements of meteorological variables using different instruments were described in the following sub-sections.

### 4.2 Urban meteorological station (CZU)

The urban meteorological station located in the capital of the Czech Republic - Prague at the west part called Suchbátov. Elevation at the station is approximately 280 m a. s. l., (50°13N, 14°37 E, Figure 8). The annual average air temperature is around 9 °C, average annual precipitation total approximately 500 mm. Spring frosts tend to linger on from 12 to 14 May, which shortens the growing season and affect the yield and productivity, especially of the fruit trees and crop plants. Summer arrives in the second half of June with warmer weather. Average temperature in July achieves above 19 °C. The average growing season with 2800 - 3000 degree-days (sum of average daily air temperatures 10 °C at least) extends for around 165 to 180 days, from the second half of April to the first half of October. Nearly 40 percent of the annual total precipitation falls from June to September (CZU, 2020). This meteorological

station provides the official meteorological data for the university. Being originally located in open field according to requirements for a standard meteorological station, within the CZU campus development is the station now surrounded by tall buildings and concrete parking lots. Progress in construction during the study period is documented in Appendix 1.

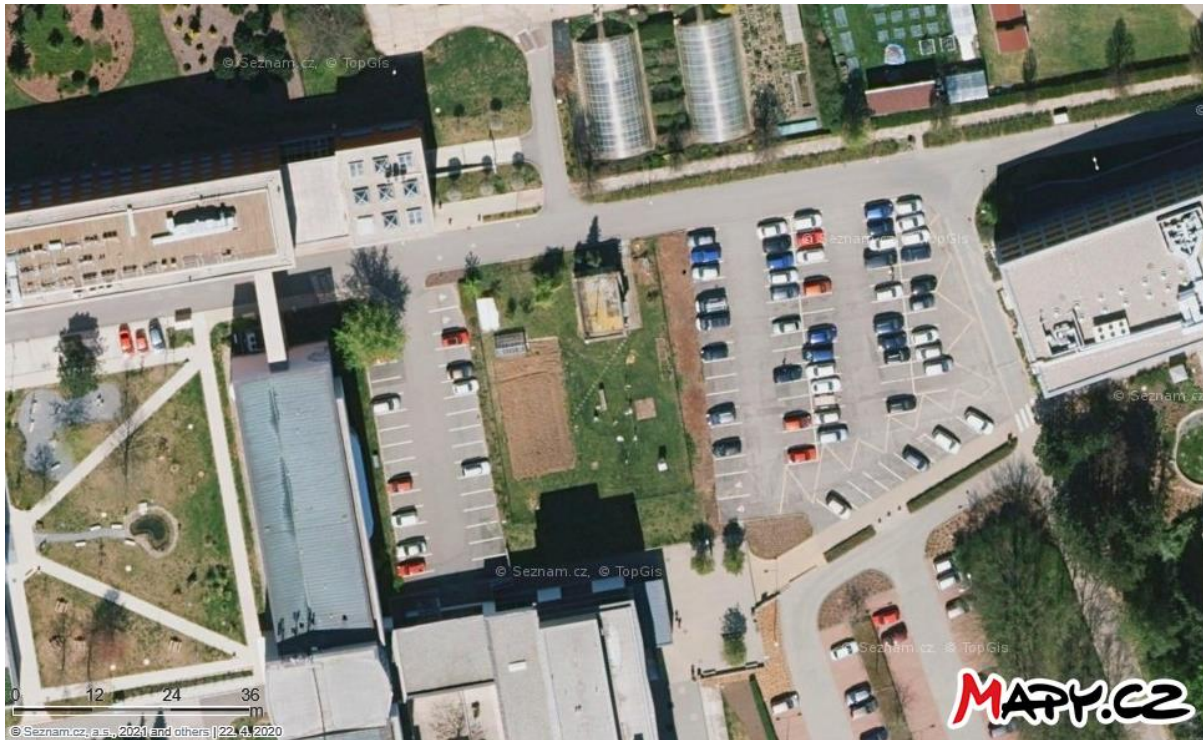


Figure 8 CZU meteorological station representing the urban conditions (<https://en.mapy.cz/>).

### 4.3 Rural meteorological station (DWR)

Measurement of meteorological variables were carried out at the station of the Department of Water Resources, with the geographical location of  $14^{\circ} 23'0''\text{E}$  and  $50^{\circ} 08'0''\text{N}$  and 286 m a.s.l (Mekonnen et al., 2015) (Fig. 11). The climate of this site is moderately warm and moderately dry, receiving the average annual temperature of  $9.1^{\circ}\text{C}$  and precipitation total about 495 mm, respectively. The surrounding land area of the weather station is used as arable land with maize parcel belonging to a long-term stationary experiment which was started in 1992. Within the weather station, there are instruments on masts set up for recording wind speed and direction (at 10 m), dry and wet bulb temperature (at 2 m), ground temperature, visibility and wind speed (at 2 m), air humidity sensor and pyranometer and some others (Doležal et al. 2015; Doležal et al. 2018). While the CZU station surrounding was subjected to changes during the study period, the surrounding of DWR station remained the same, with one low building in close vicinity, just the trees were growing in time. Pictures from different years are in Appendix 2.





Figure 9 DWR Meteorological station (<https://en.mapy.cz/>)

#### 4.4 Observation of meteorological variables

The comparison of observations from the two stations was carried out in period 2013–2020, as data were available for these years. Only the month June was investigated from each year. June was selected, as there was an assumption of the biggest differences in variables, because in this month are generally recorded the highest values of global radiation, the Sun is at the highest position and the air is cleanest, which affects the radiation components ratio. In other months the diffuse component is higher.

The meteorological variables used for analysis were air pressure, air temperature including temperature extremes, air humidity at 2 m above the ground, wind speed and direction at 10 m above the ground and daily precipitation totals recorded with various instruments based on previous installation of both weather stations.

The data of urban station (CZU) were extracted from (<http://meteostanice.agrobiologie.cz/>) in 15 min interval (air temperature, air humidity, air pressure, global radiation, wind speed and wind direction) or as daily values (precipitation and temperature extremes). Data of rural station (DWR) were obtained as raw outputs either as Excel sheets downloaded from WinMeteo software (air temperature, air humidity, precipitation) or in native dbd format from dataTaker DT80 and extracted using the dPlot software (global radiation, wind speed and wind direction), all data in 10 min interval. Due to technical problems, there were gaps in data from

data Taker in years 2013, 2017-2020. Thus, range of those data from CZU station was adjusted to be comparable. The numbers of complete days suitable for comparison between 2013-2020 were 12, 30, 30, 30, 29, 29, 23, 16, respectively. There is no information about air pressure from DWR station, however, this variable is not considered to be affected by urbanization.

#### **4.4.1 Measurement of air humidity**

Humidity measurements at the Earth's surface are required for various application in agriculture, hydrology, environment and meteorological analysis and forecasting, for climate studies, in general. The measurement of air humidity play an important role for climate record relevance to the changes of state of water in the atmosphere. The units and symbols generally used for air humidity or relative humidity is in percentage (Kanniah et al. 2012). The air humidity at DWR was measured by a combined probe HMP 45A/D (Vaisala) (Doležal et al. 2018) and by HMP45C relative humidity probe, VAISALA, Finland at CZU station.

#### **4.4.2 Measurement of air pressure**

The atmospheric pressure on a given surface is the force exerted per unit area by the weight of the Earth's atmosphere above. Atmospheric pressure is an important parameter for studying weather of a location and its interaction with the crops. Air pressure was measured using the RPT410F pressure sensor, CS, UK, at the CZU station only.

#### **4.4.3 Measurement of air temperature**

The temperature sensor was set up at weather station and mounted 2 m above the ground surface without shielding against wind effects. A computer stationed at the field was dedicated to monitoring the pulse generated by a contact closure, and the 10 min air temperature were recorded from the month of June from 2013-2020 (00:00 AM to 23:50 PM CET) of DWR meteorological station by a combined probe HMP 45A/D (Vaisala), Doležal et al. (2018). Daily minima and maxima further referred as temperature extremes were extracted from the values. On the other hand, the data collection from CZU meteorological station have been downloaded from the web site (<http://meteostanice.agrobiologie.cz/>) in the whole month of June from 2013-2020 with 15 mins of temporal resolution (00:15 AM to 23:59 PM CET) by thermometer model PT100/3 1/3 DIN PT100 installed on the spot.

#### **4.4.4 Daily precipitation totals**

Precipitation denotes all forms of water (liquid or solid) that reach the earth from atmosphere. Precipitation includes rain, snow, hail, dew, fog, drizzle etc., of all these only rain and snow

contribute significant amount of water on the earth. The amount of daily precipitation of urban area (CZU) was measured by Rain gauge model SR03 (Figure 10).

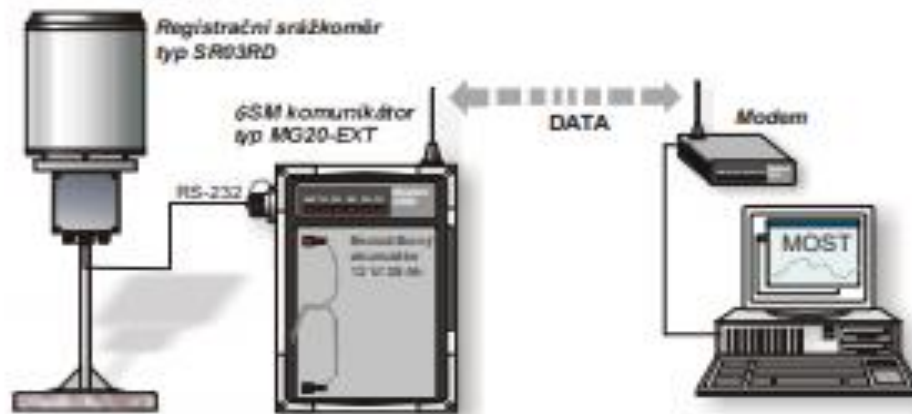


*Figure 10 Rain gauge precipitation record Model SR03*

The daily precipitation totals of DWR Station was recorded using a 0.01” heated tipping-bucket rain gauge MR3H (Meteoservis, v.o.s, Vodňany) placed at the experimental site, with its upper rim at 1.00 m above the ground with Ten- minutes of time interval (Doležal et al. 2018).



*Figure 11 MR3H tipping-bucket rain gauge (TBR-MR3H)*

#### 4.4.5 Measurement of wind speed and direction

Wind plays an important role in crop evapotranspiration and thus determines crop water use. The measurement of wind is thus necessary for studying the crop growth (Kanniah et al. 2012). The instrument used for measurement at CZU station was A100R/W200P wind speed and direction sensor, EM, UK with mounted at 2 m above the ground surface (Figure 12), and DWR rural station was using an ultrasonic sensor Windsonic (Gill Instruments Ltd.) (Doležal et al. 2018).



*Figure 12 Switching of ANEMOMETER (A100R)*

#### 4.4.6 Measurement of global radiation

Electromagnetic radiation is emitted by everything in nature and the energy emitted by the Sun is solar radiation. The solar (global downward short wave) radiation was measured by a pyranometer (LP02 Hukseflux, *Figure 13*) at the reference height of 2 m above the ground surface from DWR station (Doležal et al. 2018) and CM11 pyranometer, K&Z, NL from CZU urban meteorological station. The changes in global radiation at the top of the atmosphere due to changes in geometry, namely the daily course of the Sun and seasonal effects, are usually well reproduced by models and lead to a de facto correlation between observations and estimates hiding potential weakness of a model (Boilley et al. 2015).



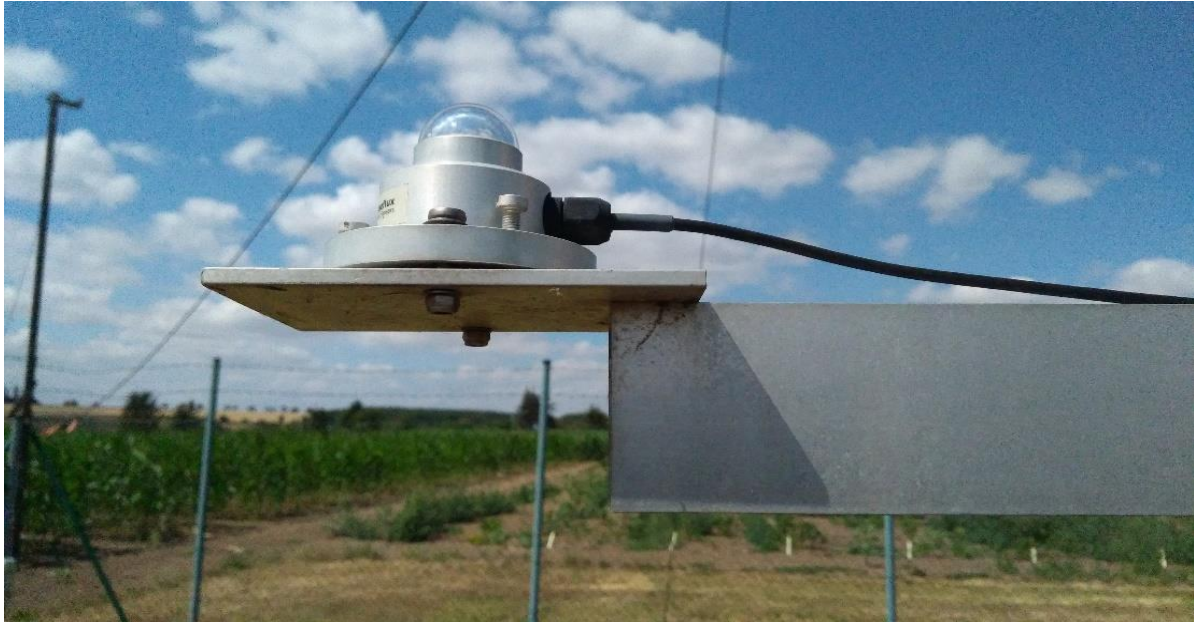


*Figure 13 Pyranometer (LP02 Hukseflux) of solar radiation record*

An et al. (2017) Global radiation consists of direct and diffuse radiations. Solar radiation spread to earth and it can be easily reach to the surface without any obstacle. Net radiation includes the absorption and reflection of short-wave radiation, as well as the outgoing and incoming long-wave radiations, and can be expressed as follows:

#### **Net solar or net shortwave radiation ( $R_{ns}$ )**

The result from the balance incoming and reflected solar radiation is given by:

$$R_{ns} = (1 - \alpha)R_s \quad (4.1)$$

Where  $R_{ns}$  net solar or shortwave radiation ( $\text{MJ m}^{-2} \text{day}^{-1}$ ),  $\alpha$  is the soil surface albedo ( $\alpha = 0 - 1$ )  $R_s$  the incoming solar radiation ( $\text{MJ m}^{-2} \text{day}^{-1}$ )

#### **Net longwave radiation ( $R_{nl}$ )**

Water vapour, clouds, carbon dioxide and dust are both absorb and emit of long wave. However, the rate longwave energy. The Stefan-Boltzmann law used for expressed the relationship quantity. The net energy flux leaving the earth's surface is, however, less than that emitted and given by the Stefan-Boltzmann law due to the absorption and downward radiation from the sky. Their concentrations should be known when assessing the net outgoing flux.

The Stefan-Boltzmann law is corrected humidity and cloudiness when estimating (Allen et al. 1998).

The net outgoing long wave radiation from a grassed soil surface is estimated as:

$$R_{nl} = \sigma \left( \frac{T_{min}^4 + T_{max}^4}{2} \right) (0.34 - 0.14 \sqrt{e_a}) \left( 1.35 \frac{R_s}{R_{so}} - 0.35 \right) \quad (4.2)$$

Where:

- $R_{nl}$  net outgoing longwave radiation ( $\text{MJ m}^{-2} \text{ day}^{-1}$ ),
- $\sigma$  Stefan-Boltzmann constant ( $4.903 \cdot 10^{-9} \text{ MJ K}^{-4} \text{ m}^{-2} \text{ day}^{-1}$ )
- $T_{max}$ ,  $T_{min}$ , maximum and minimum air temperature ( $^{\circ}\text{C}$ )
- $e_a$  actual vapour pressure (kPa)
- $R_s/R_{so}$  relative shortwave radiation (limited to  $\leq 1.0$ ),
- $R_s$  measured solar radiation ( $\text{MJ m}^{-2} \text{ day}^{-1}$ )
- $R_{so}$  clear-sky radiation ( $\text{MJ m}^{-2} \text{ day}^{-1}$ )

$$R_a = \frac{24(60)}{\pi} G_{sc} d_r [\omega_s \sin(\varphi) \sin(\delta) + \cos(\varphi) \cos(\delta) \sin(\omega_s)] \quad (4.3)$$

where

- $R_a$  extraterrestrial radiation in the hour ( $\text{MJ m}^{-2} \text{ hour}^{-1}$ )
- $G_{sc}$  solar constant =  $0.0820 \text{ MJ m}^{-2} \text{ min}^{-1}$
- $d_r$  inverse relative distance Earth-Sun
- $\delta$  solar declination (rad)
- $\varphi$  latitude [rad] (Equation 22),
- $\omega_1$  solar time angle at beginning of period (rad)
- $\omega_2$  solar time angle at end of period (rad)

### ***Net radiation ( $R_n$ )***

The net radiation ( $R_n$ ) is the difference between the incoming net shortwave radiation ( $R_{ns}$ ) and the outgoing net longwave radiation ( $R_{nl}$ ):

$$R_n = R_{ns} - R_{nl} \quad (4.4)$$



## **4.5 Statistical analysis**

In order to compare the datasets measured in different time intervals (10 or 15 min), hourly or daily average or sum were calculated. Data were processed in MS Excel.

To test the measurement precision and accuracy of the meteorological variables measured by several sensors and registered by several reading devices in their response to different meteorological station and variables, a one-way and factorial analysis of variance (ANOVA); Duncan's Test with  $p < 0.05$  were performed using Statistica version 13.5.0.17 (TIBCO Software Inc.) software package to test the statistical differences.

The correlation coefficient ( $r$ ) and correlation plots were employed to estimate the statistical relationship to indicate the strength of the relationship between the two different meteorological stations (Schober et al. 2018).

## 5 Results

### 5.4 Air humidity

Variation of air humidity hourly average shows in Figure 14 the CZU and DWR meteorological data recorded from 2013-2020. The result showed that the combined effect of year and station between CZU and DWR meteorological stations is not significantly significant ( $P\_value > 0.05$ ). However, the graph showed that the hourly average of air humidity of DWR meteorological station is statistically significantly lower than CZU meteorological station. The value of air humidity in hourly average in 2013 had the highest value and the lowest was in 2019. Table 2 shows that temporal record of air humidity in hourly average is significantly different ( $P\_value < 0.05$ ) in period study from 2013-2020 of both meteorological stations. The scatter plots of temporal trends of the measured data during the study period in Fig. 15 below show the similar trend of relationship between both station data.

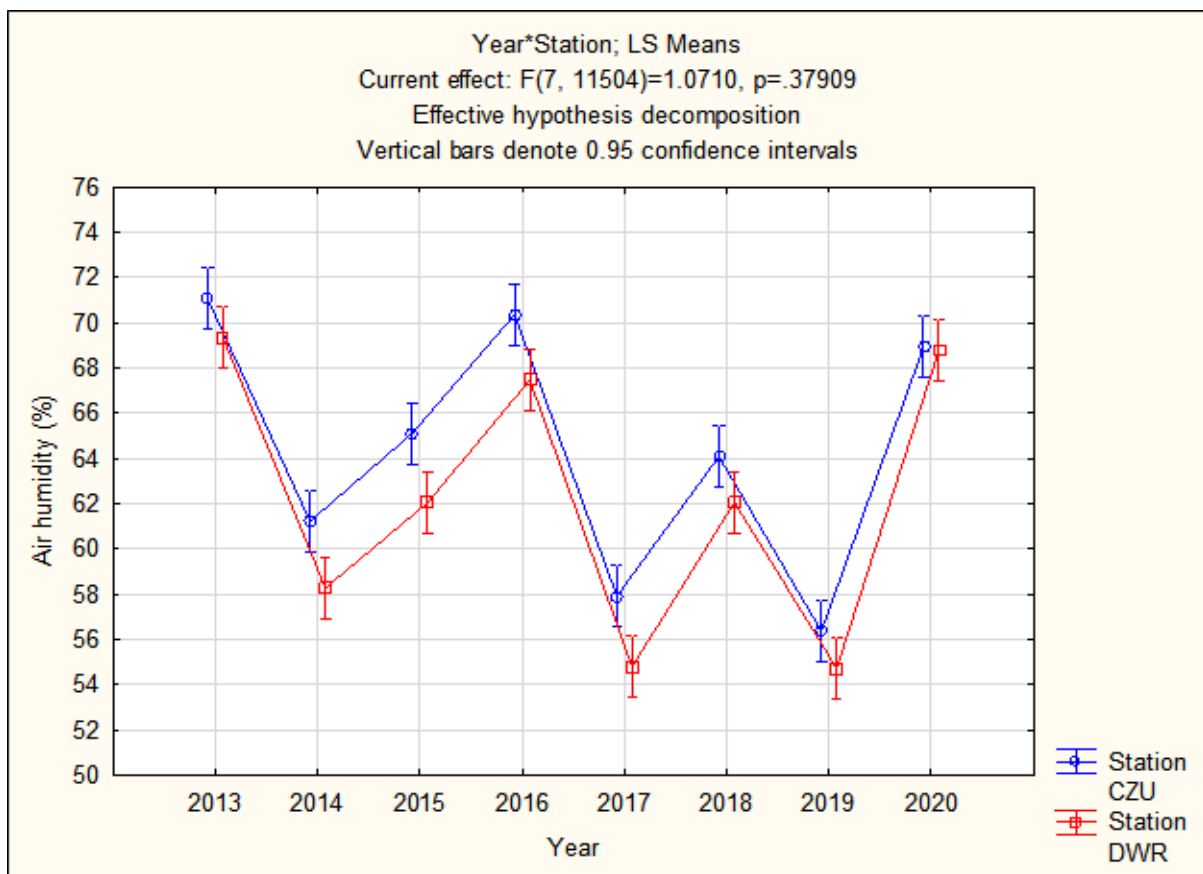


Figure 14 Temporal variation of air humidity in hourly average

Table 2 Hourly average of air humidity observed from CZU and DWR station according to ANOVA in Statistica ( $P < 0.05$ ).

Effect	Univariate Tests of Significance for Air humidity (%) in peak hour Sigma-restricted parameterization Effective hypothesis decomposition				
	SS	Degr. of	MS	F	p
Intercept	46134987	1	46134987	130658.8	0.000000
Year	333297	7	47614	134.8	0.000000
Station	13918	1	13918	39.4	0.000000
Year*Station	2647	7	378	1.1	0.379092
Error	4062006	11504	353		

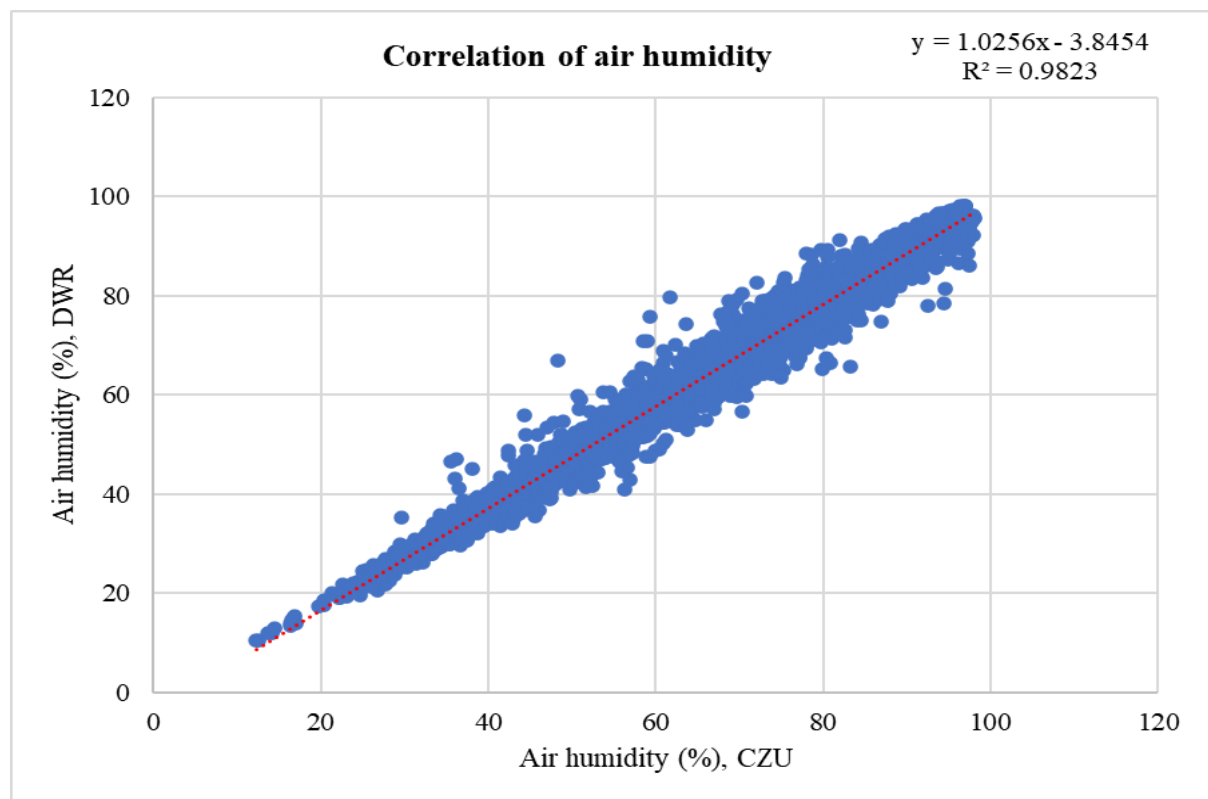


Figure 15 Scatter plot of air humidity hourly average from CZU and DWR meteorological station

Table 3 summarizes the hourly average of air humidity from 2013 to 2020 of CZU and DWR meteorological station. It demonstrated that the hourly average of air humidity in 2013 of CZU and DWR stations had highest value 71.01%, 69.34%, while standard deviation was 17.07%, 17.72%, respectively. However, in 2019 had the lowest of hourly average of air humidity of both CZU and DWR stations were about 56.36%, 54.71%, while standard deviations were 19.91%, 20.65%, respectively.

Table 3 Overall statistic of air humidity hourly average.

Station	Year	mean	stdev	CV	min	max	median	skewness	kurtosis
CZU	2013	71.07	17.07	24.02	31.23	94.58	73.71	-0.38	-1.07
	2014	61.22	18.09	29.54	23.58	93.35	62.01	-0.07	-1.12
	2015	65.11	17.84	27.39	27.15	94.55	65.70	-0.21	-1.02
	2016	70.37	17.59	25.00	28.23	96.55	73.93	-0.39	-1.01
	2017	57.91	20.40	35.23	22.08	97.53	56.18	0.23	-1.03
	2018	64.10	17.97	28.04	26.70	98.03	64.45	-0.05	-0.95
	2019	56.36	19.91	35.33	12.23	95.75	55.48	0.10	-0.90
	2020	68.94	18.82	27.30	30.60	96.98	71.38	-0.27	-1.12
DWR	2013	69.34	17.72	25.56	28.17	93.00	72.33	-0.40	-1.08
	2014	58.27	18.72	32.12	19.67	92.50	59.17	-0.05	-1.12
	2015	62.04	18.49	29.80	23.50	93.00	62.58	-0.18	-1.05
	2016	67.47	17.92	26.56	22.50	94.00	70.58	-0.37	-0.98
	2017	54.79	20.54	37.49	19.00	94.33	53.33	0.21	-1.07
	2018	62.10	18.39	29.61	23.83	96.00	62.67	-0.09	-0.99
	2019	54.71	20.65	37.74	10.50	96.00	53.83	0.10	-0.99
	2020	68.77	20.01	29.10	27.33	98.00	71.75	-0.31	-1.13

Figure 16 demonstrated the diurnal difference of air humidity of CZU and DWR meteorological stations. It shows that combined effect of both station and year was not significantly different ( $P\_value > 0.05$ ), however, years differ statistically significantly and both stations, too. The highest difference was in 2019 following with 2017 and 2014 and the lowest difference was in 2013. Figure 17 the trends relationship of diurnal difference of air humidity showed that DWR meteorological station was higher than CZU meteorological station.

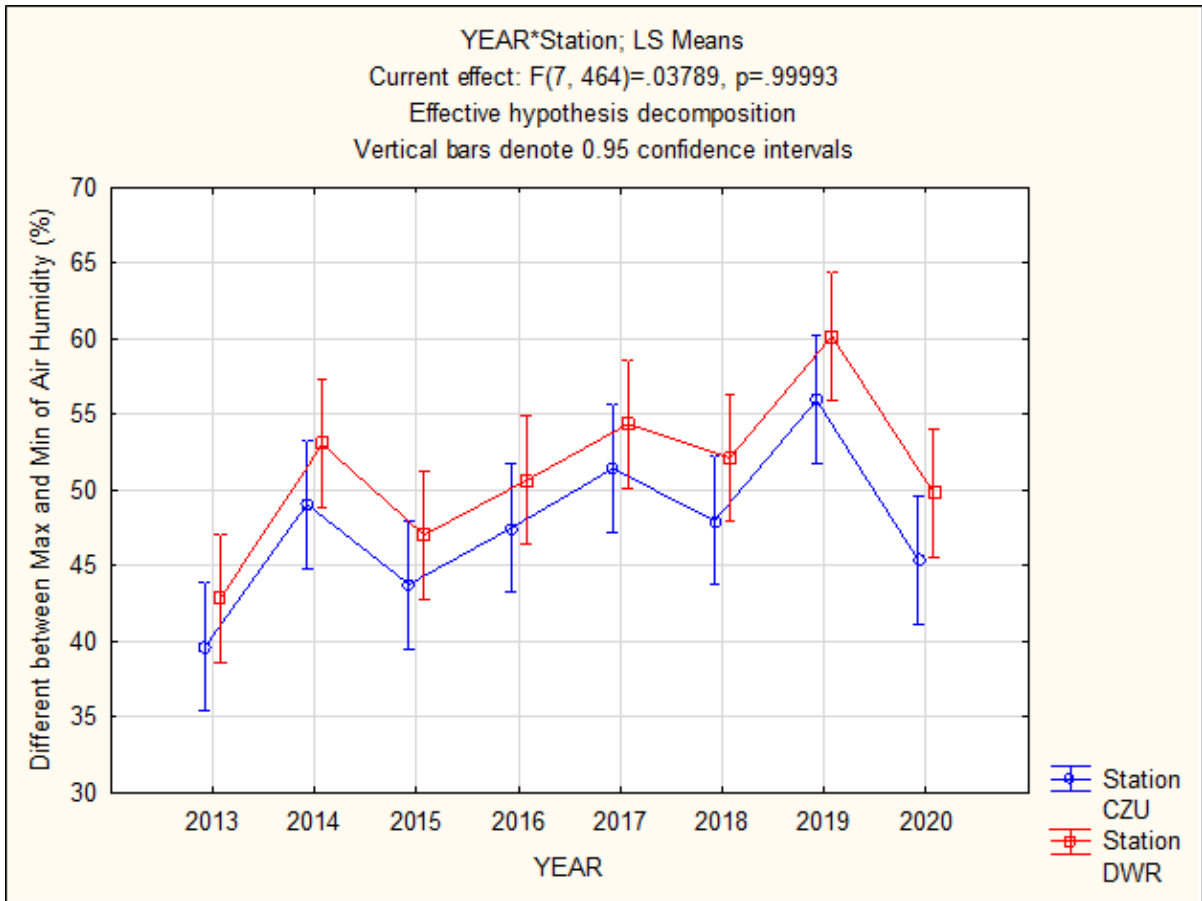


Figure 16 Air humidity diurnal difference between CZU and DWR meteorological station

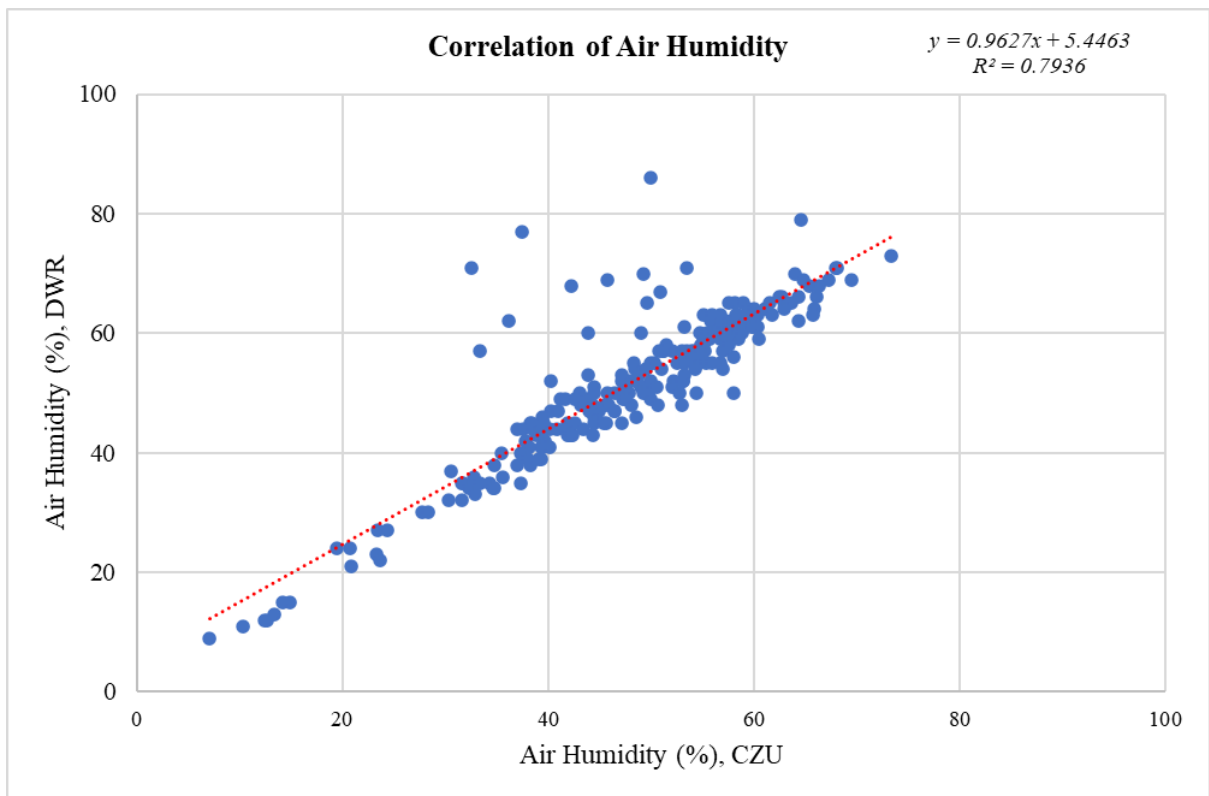


Figure 17 Scatter plot Relationship of air humidity diurnal difference

## 5.5 Air pressure

Figure 20 showed the hourly average of air pressure of CZU meteorological station measured by barometric pressure sensor. According to ANOVA the comparison between 2013 until 2020 were significantly different ( $P\_value < 0.05$ ) the air pressure of hourly average from 2013 to 2014 was rising slightly. However, the amount of air pressure from 2014 to 2015 dramatically change then falling from 2015 to 2016. Therefore, the value of air pressure from 2016 until 2019 go up from year to year then falling gradually in 2020. Table 4 summarizes hourly average of air pressure indicating that 2015 had the highest of air pressure 985.11 hPa, with standard deviation 4.89 hPa, respectively. However, the lowest air pressure was in 2020 about 979.33 hPa, with standard deviation 6.17 hPa, respectively. There is no information of air pressure record of DWR meteorological station. The reason is different weather conditions determined by synoptic situations (distribution of pressure formations) over Central Europe, which are often very different in individual years. The reason is the fact that the Czech Republic is in a transitional climate, where the influence of both the ocean and the continent is exercised.

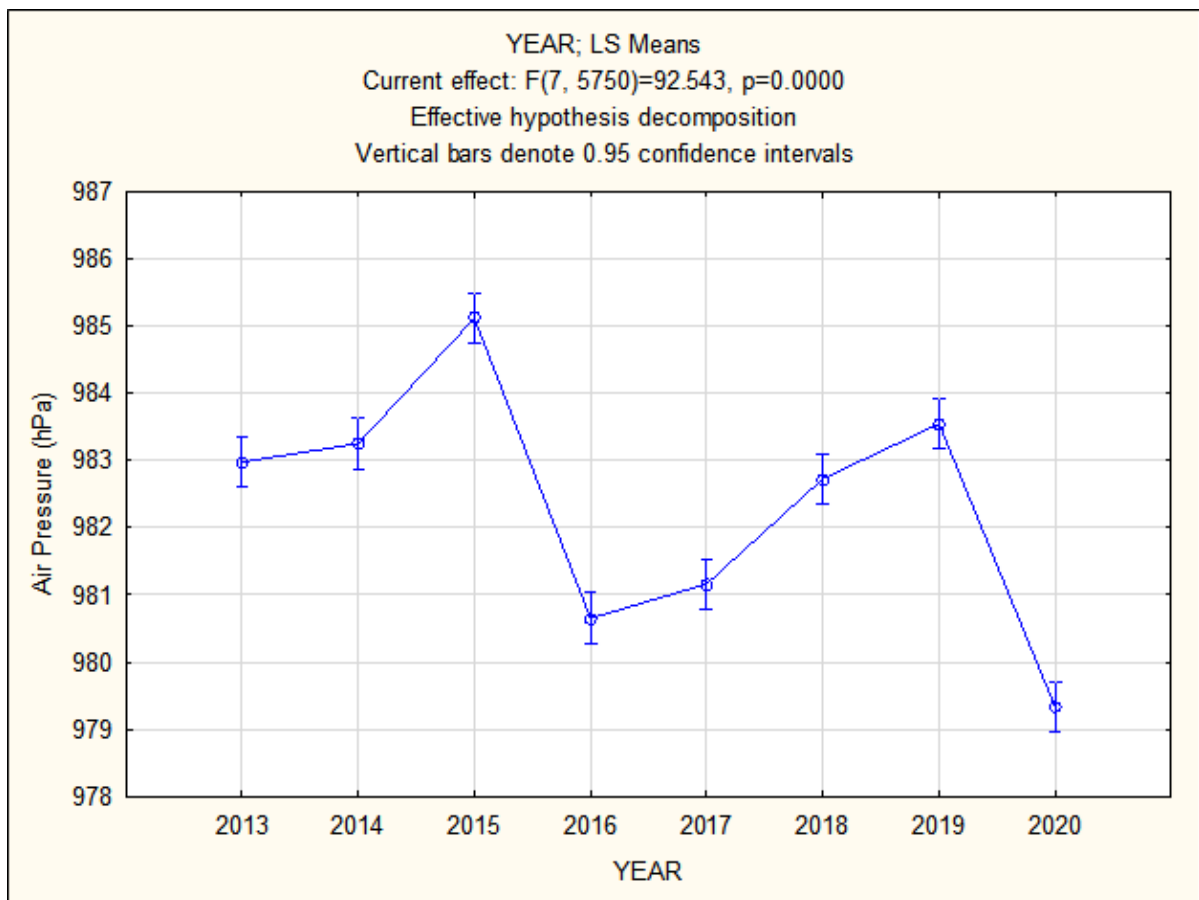


Figure 18 Temporal air pressure hourly average from 2013-2020

*Table 4 Summary of statistical information of air pressure in hourly average*

Station	Year	mean	stdev	CV	min	max	median	skewness	kurtosis
CZU	2013	982.98	4.28	0.44	971	991	984	-0.85	0.58
	2014	983.25	3.44	0.35	974	991	984	-0.53	-0.05
	2015	985.12	4.89	0.50	971	995	986	-0.44	-0.52
	2016	980.65	6.49	0.66	966	992	981	-0.46	-0.43
	2017	981.17	6.16	0.63	959	992	982	-1.12	1.67
	2018	982.73	3.96	0.40	973	990	983	-0.15	-0.78
	2019	983.55	4.90	0.50	972	992	984	-0.28	-1.01
	2020	979.33	6.17	0.63	961	991	980	-0.57	0.75

## **5.6 Air temperature**

Figure 19 shows the temporal variability of air temperature in hourly average at 2 m above the ground surface of CZU and DWR meteorological stations. The comparison of air temperature in hourly average between CZU and DWR meteorological station was not significantly different ( $P\_value > 0.05$ ), however, it is higher at DWR in all years. The result indicated that hourly average of air temperature in 2019 was dramatically high and the lowest temperature in hourly average was in 2013 then following with 2014 and 2015. Table 5 demonstrates the temporal record of air temperature in hourly average in period study from 2013-2020 of each meteorological station was significantly different ( $P\_value < 0.05$ ). Figure 20 scatter plot relationship of air temperature of CZU and DWR meteorological station shows similar trend.

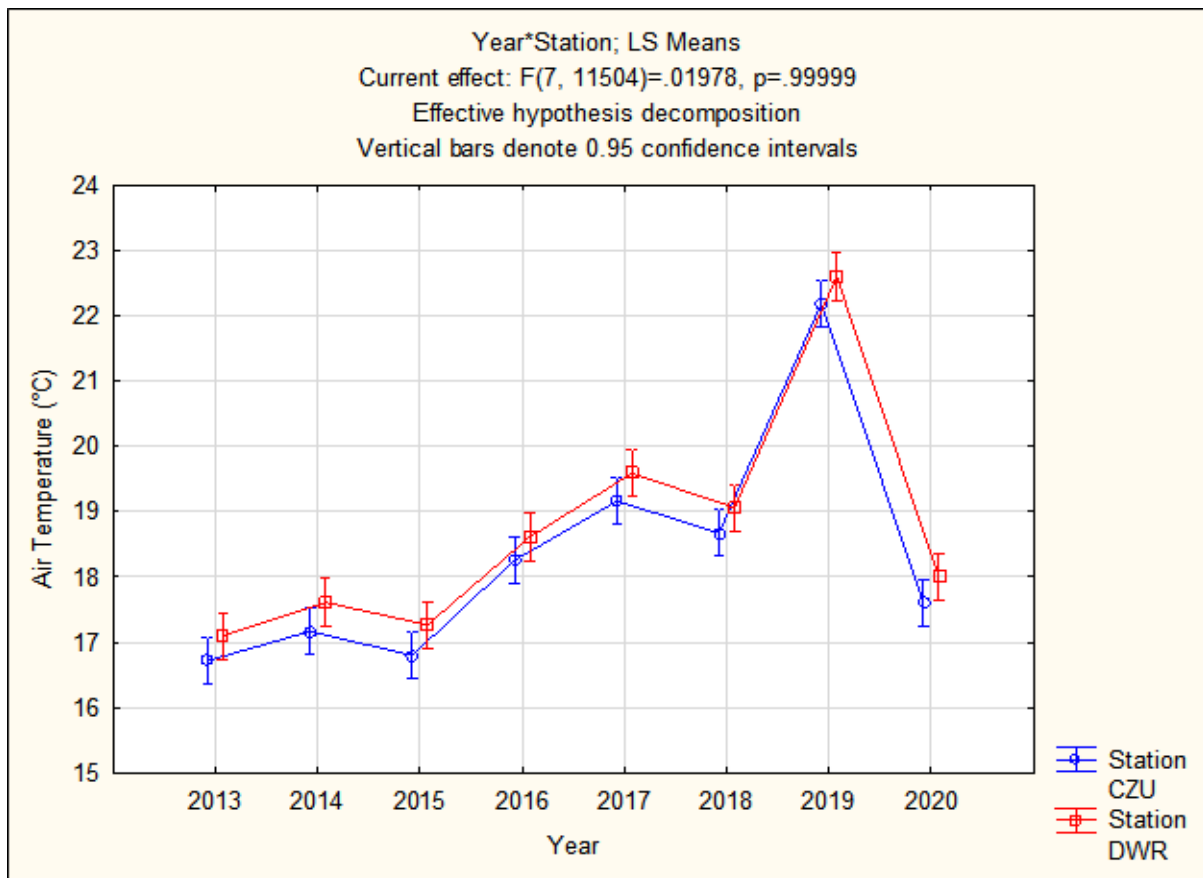
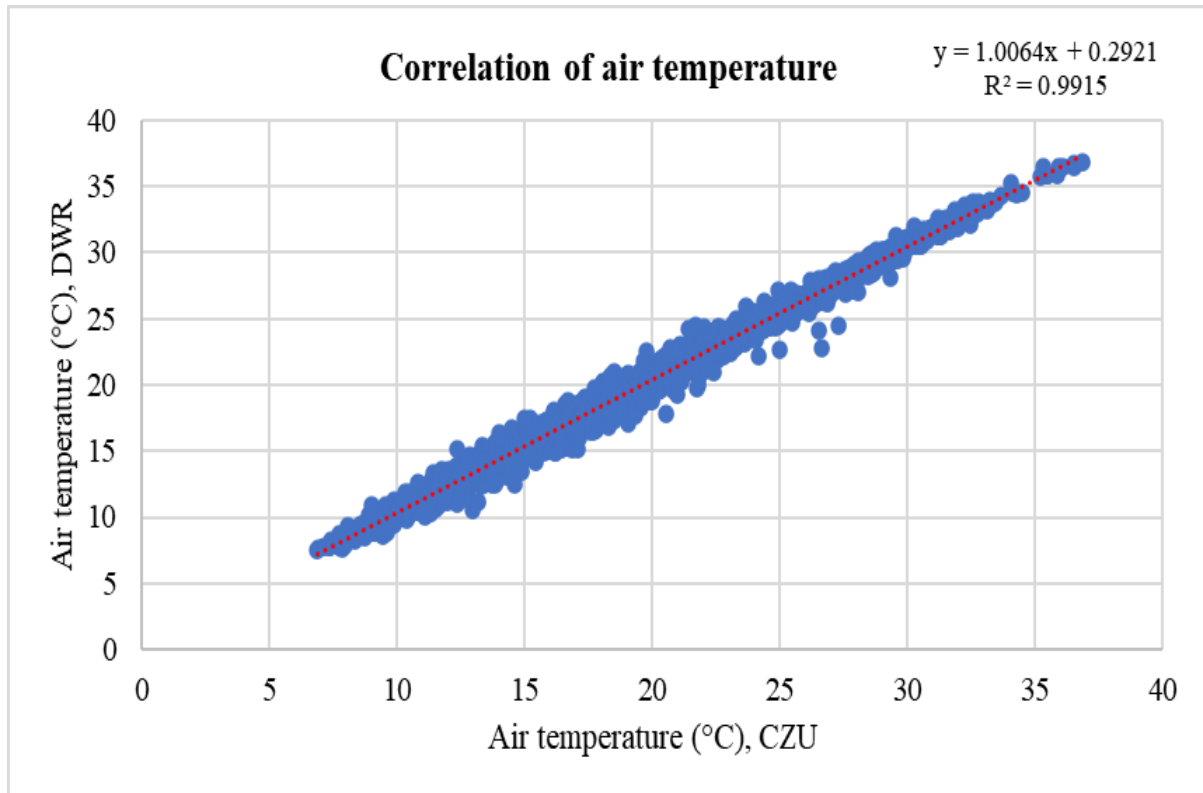


Figure 19 Temporal variation of air temperature in hourly average at 2 m

Table 5 ANOVA of air temperature in hourly average

Univariate Tests of Significance for Air Temperature (°C) in the peak hour					
Sigma-restricted parameterization					
Effective hypothesis decomposition					
Effect	SS	Degr. of	MS	F	p
Intercept	3954018	1	3954018	163056.2	0.000000
Year	32309	7	4616	190.3	0.000000
Station	482	1	482	19.9	0.000008
Year*Station	3	7	0	0.0	0.999993
Error	278965	11504	24		





*Figure 20 Scatter plot illustrating the relationship of air temperature hourly average*

Table 12 shows the summary of statistical information of air temperature in hourly average of both meteorological stations. The result showed that the highest value of hourly average of air temperature was in 2019 in period study from 2013-2020 of both CZU and DWR meteorological stations about 22.18 °C, 22.60 °C, with standard deviation 5.16 °C, 5.19 °C, respectively. However, the lowest hourly average of air temperature was in 2013 of CZU and DWR meteorological station were 16.72 °C, with standard deviation 5.77 °C and 17.10 °C, with standard deviation 5.85 °C, respectively. Therefore, the maximum and minimum of air temperature record of CZU meteorological station were 36.88 °C in 2019 and 7.15 °C in 2015. The maximum and minimum of DWR were 36.85 °C in 2019 and 7.52 °C in 2013.

*Table 6 Descriptive statistics of air temperature in hourly average between CZU and DWR station*

Station	Year	mean	stdev	CV	min	max	median	skewness	kurtosis
CZU	2013	16.72	5.77	34.51	6.88	33.23	15.61	0.70	-0.08
	2014	17.17	5.09	29.65	7.75	32.23	16.53	0.84	0.54
	2015	16.80	4.92	29.30	7.15	31.23	16.16	0.56	-0.28
	2016	18.26	4.30	23.56	10.55	32.23	17.49	0.81	0.40
	2017	19.16	5.03	26.25	8.35	33.65	18.58	0.31	-0.49
	2018	18.67	4.62	24.77	8.83	30.48	18.23	0.26	-0.70
	2019	22.18	5.16	23.24	9.45	36.88	22.05	0.30	-0.41
	2020	17.60	4.06	23.07	9.43	29.58	17.09	0.50	-0.17
DWR	2013	17.10	5.85	34.21	7.52	33.95	16.04	0.72	-0.03
	2014	17.61	5.18	29.40	8.15	32.92	16.86	0.78	0.39
	2015	17.27	4.96	28.73	7.78	31.95	16.57	0.56	-0.29
	2016	18.61	4.38	23.51	10.63	32.58	17.81	0.79	0.31
	2017	19.59	5.08	25.94	8.20	34.23	19.02	0.32	-0.45
	2018	19.06	4.69	24.58	8.85	30.57	18.53	0.22	-0.75
	2019	22.60	5.19	22.97	9.80	36.85	22.43	0.29	-0.47
	2020	18.00	4.11	22.83	10.03	29.62	17.53	0.50	-0.24

The diurnal difference of air temperature of both meteorological station (CZU and DWR) is in Figure 21. According to analysis the diurnal difference of air temperature of CZU and DWR meteorological station were not significantly different ( $P\_value > 0.05$ ), however, when separated the effect of year and station, there are differences significant ( $P\_value < 0.05$ ). The result showed that the highest difference was in 2019 then following 2017 and lowest was 2013 and 2020. Figure 22 showing the relationship of diurnal difference of temperature of CZU and DWR meteorological station show the different trend, DWR is higher than CZU.

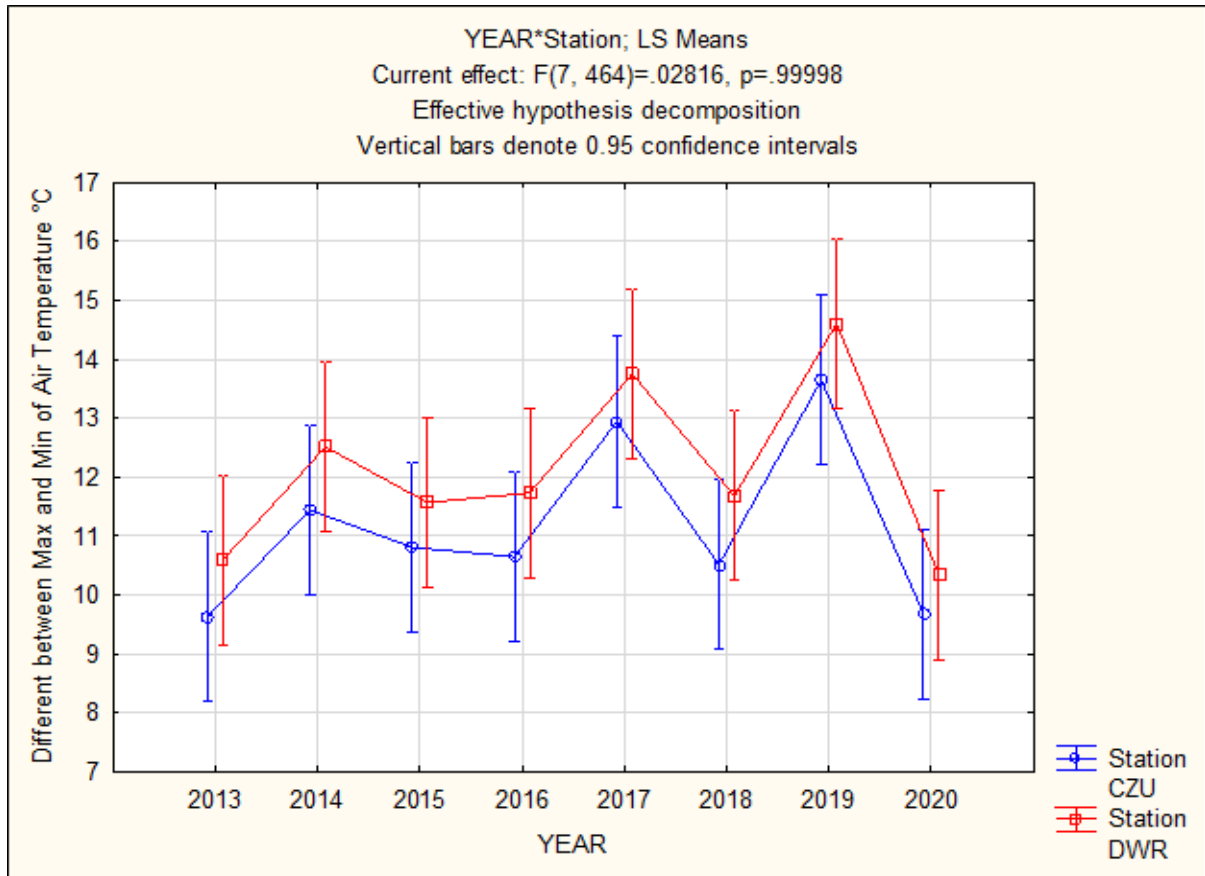


Figure 21 Time series diurnal difference of air temperature from two different weather stations

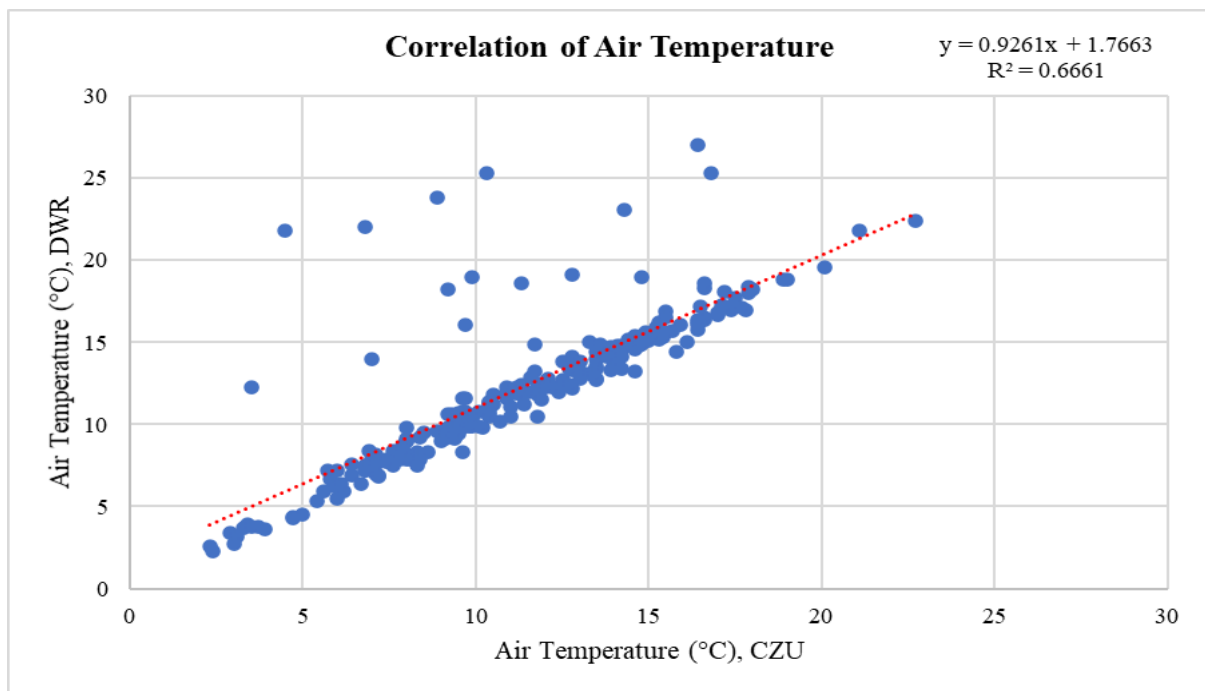


Figure 22 Scatter plot illustrating the relationship diurnal difference of air temperature

## 5.7 Temperature extreme

The variations of temperature extreme in daily average show great similarities between CZU and DWR meteorological station (**Error! Reference source not found.**). The study showed that the comparison between CZU and DWR meteorological station of temperature extreme were not significantly different ( $P\_value > 0.05$ ). The graph illustrated that in 2019 had the highest temperature extreme among the period study and the lowest record of temperature extreme was in 2013. Table 7 summary of ANOVA showed that the temperature extreme from 2013 until 2020 were not significantly different ( $P\_value < 0.05$ ) at both stations, however, at DRW is insignificantly higher. Among the year the difference is significant. Fig. 24 scatter plot of relationship between CZU and DWR meteorological data shows good correlation.

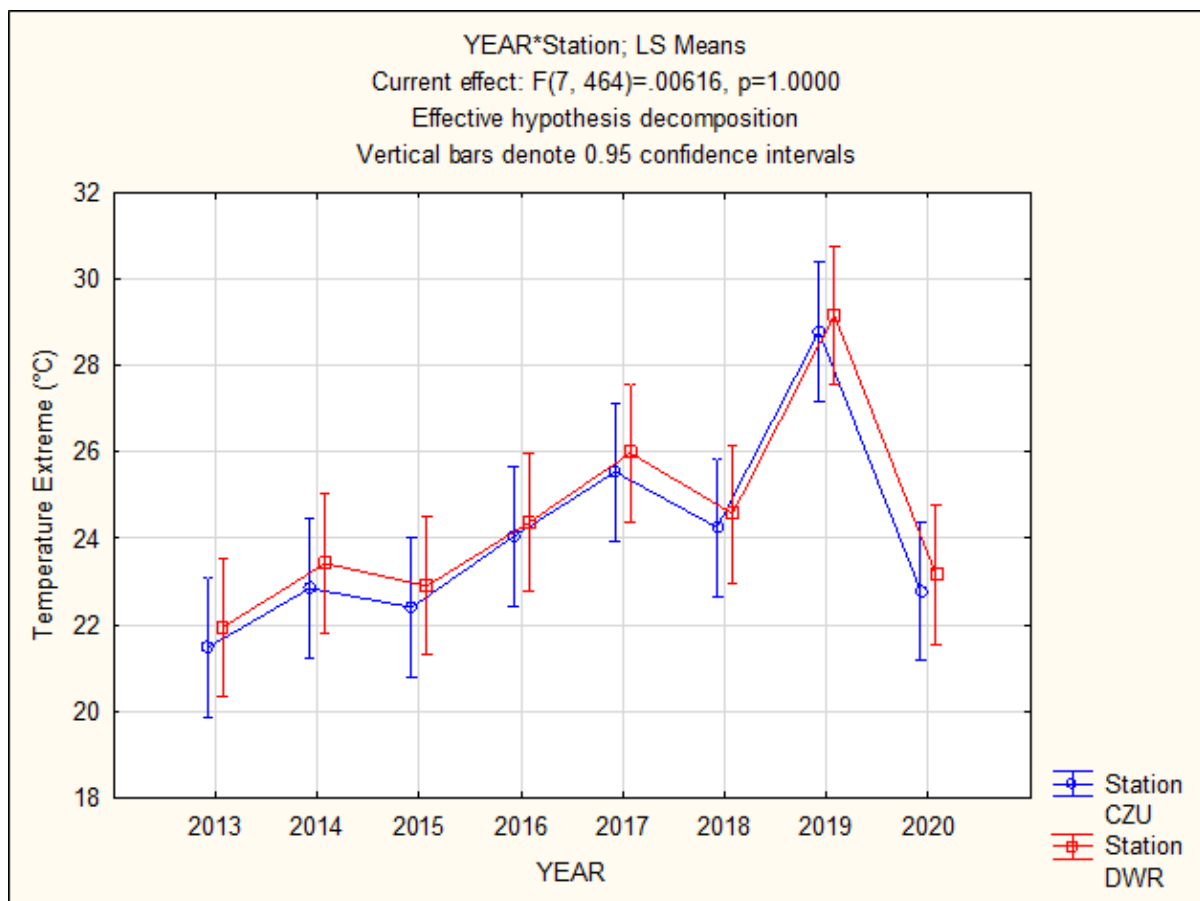


Figure 23 Historical of temperature extreme in daily average at 2 m from 2013-2020

Table 7 ANOVA of temperature extreme daily average summary

Effect	Univariate Tests of Significance for Temperature Extreme (°C) Sigma-restricted parameterization Effective hypothesis decomposition				
	SS	Degr. of	MS	F	p
Intercept	281702.8	1	281702.8	14152.83	0.000000
YEAR	2188.9	7	312.7	15.71	0.000000
Station	21.4	1	21.4	1.07	0.300569
YEAR*Station	0.9	7	0.1	0.01	1.000000
Error	9235.6	464	19.9		

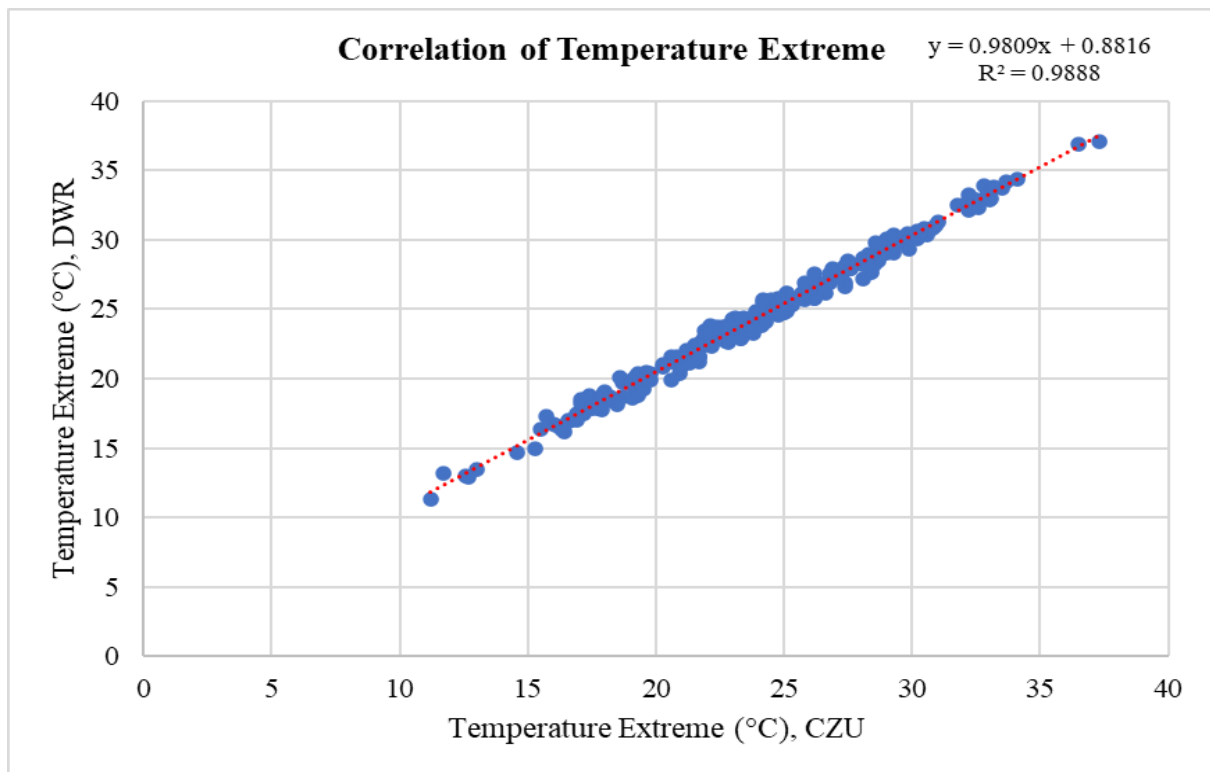


Figure 24 Scatter plot illustrating the relationship of temperature extreme daily average

Table 8 the summary of statistical information of temperature extreme in daily average. The study showed that the highest year of temperature extreme was in 2019 of CZU and DWR stations 28.78°C, 29.19 °C, with standard deviation 3.65°C, 3.54°C, respectively. However, in 2013 indicated that had the lowest of temperature extreme of CZU and DWR station 21.48°C, 21.95°C, with standard deviation 6.39 °C, 6.37 °C, respectively. The maximum of temperature extreme was in 2019 of both station CZU and DWR 37.30°C, 37.10°C. Therefore, the minimum value of temperature extreme was in 2013 of CZU and DWR station 11.20°C, 11.30°C, respectively.

Table 8 Summary of statistic of temperature extreme in daily average

Station	Year	mean	stdev	CV	min	max	median	skewness	kurtosis
CZU	2013	21.48	6.39	29.74	11.20	33.70	20.95	0.23	-0.73
	2014	22.85	4.77	20.88	16.90	32.90	21.55	1.04	0.10
	2015	22.40	4.81	21.46	12.70	31.80	21.90	0.20	-0.77
	2016	24.04	3.44	14.33	17.90	33.10	23.40	1.18	1.64
	2017	25.54	3.89	15.23	17.40	34.10	25.75	-0.09	-0.01
	2018	24.25	4.59	18.93	15.30	30.90	25.00	-0.56	-0.73
	2019	28.78	3.65	12.69	23.10	37.30	28.95	0.49	-0.07
	2020	22.77	3.64	16.00	16.60	30.20	22.75	0.16	-0.50
DWR	2013	21.95	6.37	29.01	11.30	34.20	21.55	0.30	-0.59
	2014	23.42	4.61	19.70	17.50	33.20	22.35	1.00	0.12
	2015	22.90	4.79	20.92	12.90	32.50	22.80	0.14	-0.59
	2016	24.36	3.49	14.33	17.80	33.00	23.50	1.02	1.26
	2017	25.97	3.83	14.76	17.90	34.40	26.10	0.01	0.02
	2018	24.57	4.42	18.00	15.00	31.00	25.75	-0.67	-0.57
	2019	29.16	3.54	12.13	22.90	37.10	29.50	0.39	0.01
	2020	23.16	3.66	15.79	17.00	30.10	23.15	0.06	-0.66

## 5.8 Daily precipitation totals

Figure 25 indicated the amount of daily precipitation totals recorded by CZU and DWR weather stations, measured by rain gauge. According to the analysis showing that the average daily precipitation totals between CZU and DWR meteorological station are not significantly different ( $P\_value > 0.05$ ), however, DWR reached lower values. The result showed that in 2013 both stations had the highest daily precipitation totals and from 2014 to 2020 showing that similar amount of daily precipitation. Table 9 demonstrated that daily precipitation totals between 2013 to 2020 in each year was significantly different ( $P\_value < 0.05$ ). Figure 26 illustrated very low correlation between CZU and DWR stations.

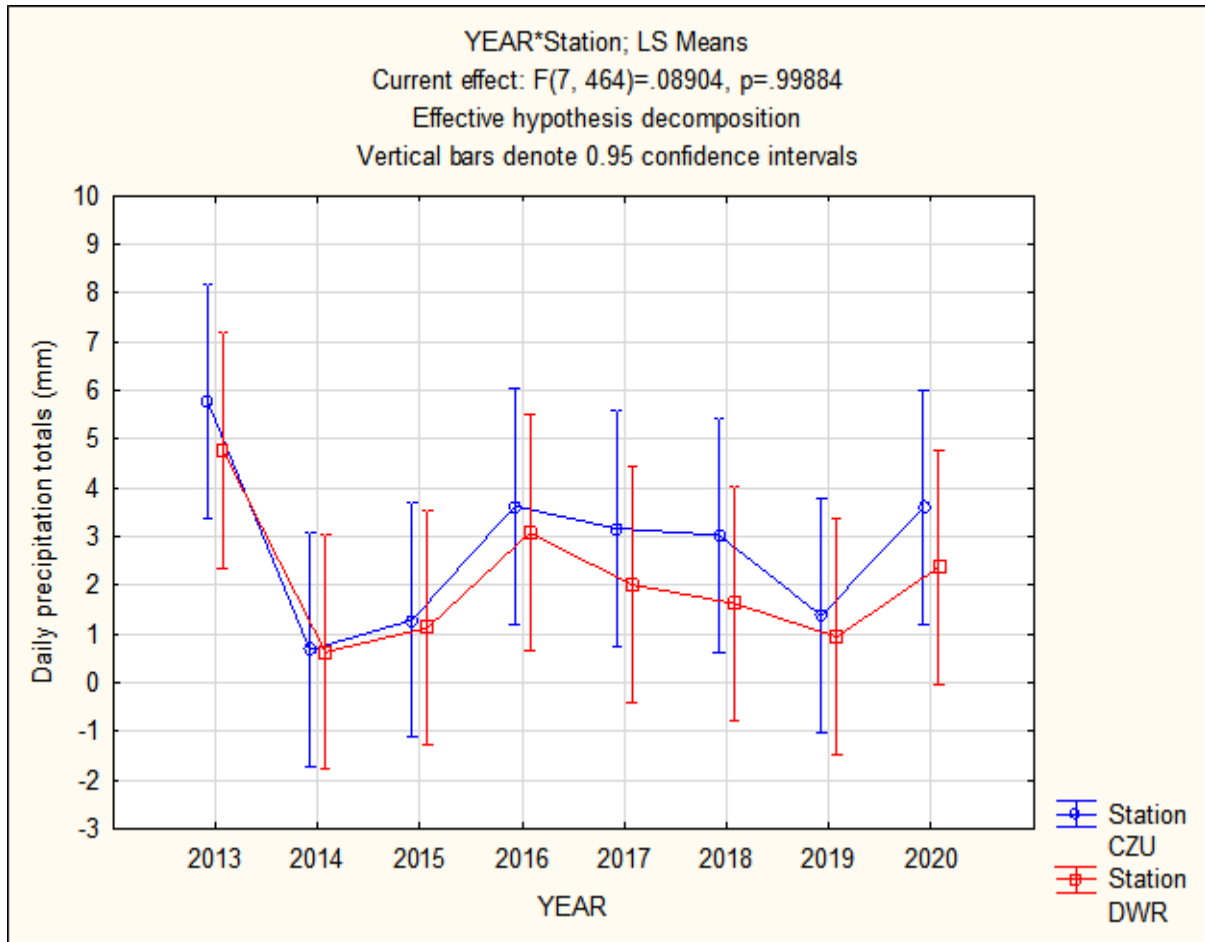
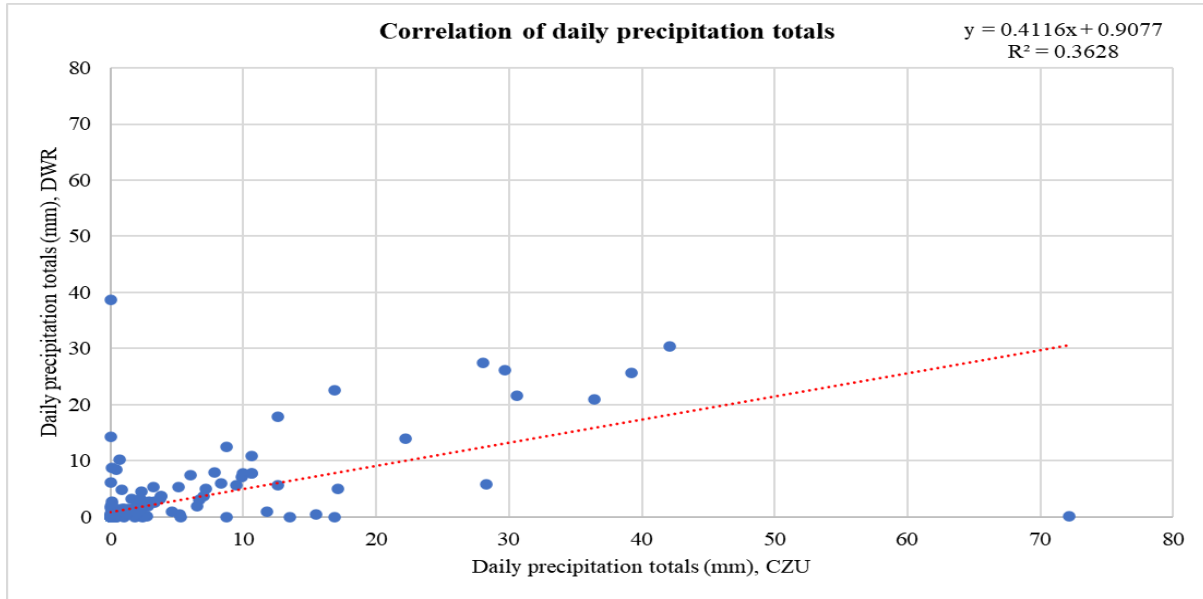


Figure 25 Average daily precipitation totals from two different weather station

Table 9 ANOVA of daily precipitation totals

Effect	Univariate Tests of Significance for Daily precipitation totals (mm) Sigma-restricted parameterization Effective hypothesis decomposition				
	SS	Degr. of	MS	F	p
Intercept	2864.08	1	2864.076	63.19138	0.000000
YEAR	932.85	7	133.265	2.94028	0.005061
Station	67.58	1	67.575	1.49094	0.222691
YEAR*Station	28.25	7	4.036	0.08904	0.998841
Error	21030.26	464	45.324		



*Figure 26 Scatter plot relationship of daily precipitation totals*

Table 10 showed that the average of daily totals of precipitation of CZU and DWR meteorological station in 2013 had highest value 5.78 mm/d, 4.46 mm/d, with a standard deviation of 14.51 mm/d, 9.31 mm/d, respectively. The maximum daily precipitation totals in 2013 was about 72.20 mm/d of CZU 2013 and 38.70 mm/d of DWR, respectively.

*Table 10 Summary statistic of daily precipitation*

Station	Year	mean	stdev	CV	min	max	median	skewness	kurtosis
CZU	2013	5.78	14.51	251.00	0.00	72.20	0.00	3.72	15.72
	2014	0.67	1.85	274.46	0.00	8.70	0.00	3.56	13.33
	2015	1.29	2.70	209.90	0.00	11.80	0.00	2.68	7.61
	2016	3.62	8.76	241.63	0.00	39.20	0.35	3.28	10.86
	2017	3.17	8.29	261.74	0.00	42.10	0.00	3.99	17.69
	2018	3.03	7.70	253.98	0.00	29.70	0.00	2.96	8.03
	2019	1.38	4.36	316.81	0.00	22.20	0.00	4.24	19.23
	2020	3.61	7.23	200.46	0.00	36.40	0.30	3.54	14.88
DWR	2013	4.76	9.31	195.47	0.00	38.70	0.05	2.33	5.45
	2014	0.63	2.30	365.78	0.00	12.50	0.00	5.05	26.54
	2015	1.12	2.52	224.62	0.00	10.20	0.00	2.59	6.17
	2016	3.08	6.79	220.55	0.00	27.50	0.20	3.06	9.07
	2017	2.01	5.77	287.21	0.00	30.40	0.00	4.42	21.55
	2018	1.63	4.87	299.25	0.00	26.20	0.05	4.76	24.25
	2019	0.94	2.77	294.33	0.00	13.90	0.00	4.00	17.52
	2020	2.37	4.36	184.08	0.00	20.90	0.55	3.02	10.95



## 5.9 Global radiation

Figure 27 illustrated the temporal variation of the global radiation from two different meteorological station. The value derived from pyranometer with daily records. The result showed that the daily amount of global radiation from CZU and DWR meteorological station was not significantly different ( $P\_value > 0.05$ ). The study indicated that in 2019 the amount of global radiation was dramatically high from both stations and in 2020 was dramatically low.

Figure 28 shows that the amount of global radiation between daytime of CZU and DWR meteorological station was significantly different ( $P\_value < 0.05$ , Table 11). The amount of global radiation in morning (am) was higher at the DWR station than at CZU station, and in the afternoon it was opposite. It is well illustrated in Figure 29 where are records from four clear days in 2014 with low variations. However, the global radiation of CZU was slightly different between morning and afternoon.

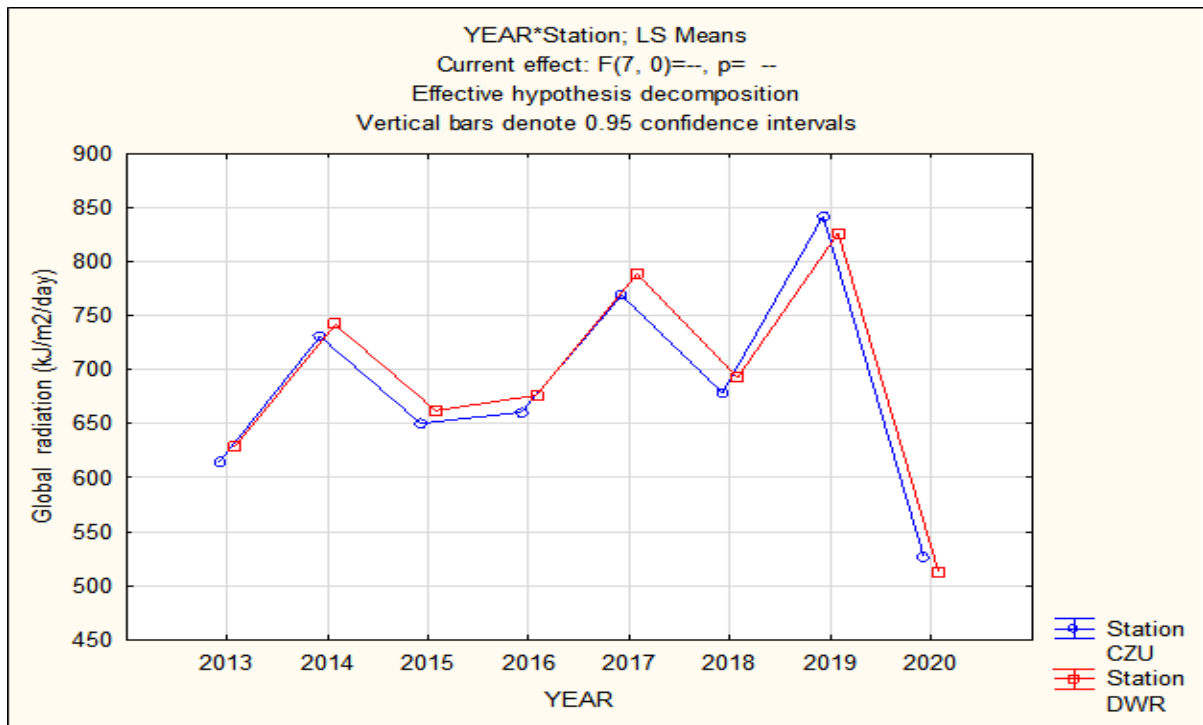


Figure 27 Historical of solar radiation hourly average from (2013-2020)

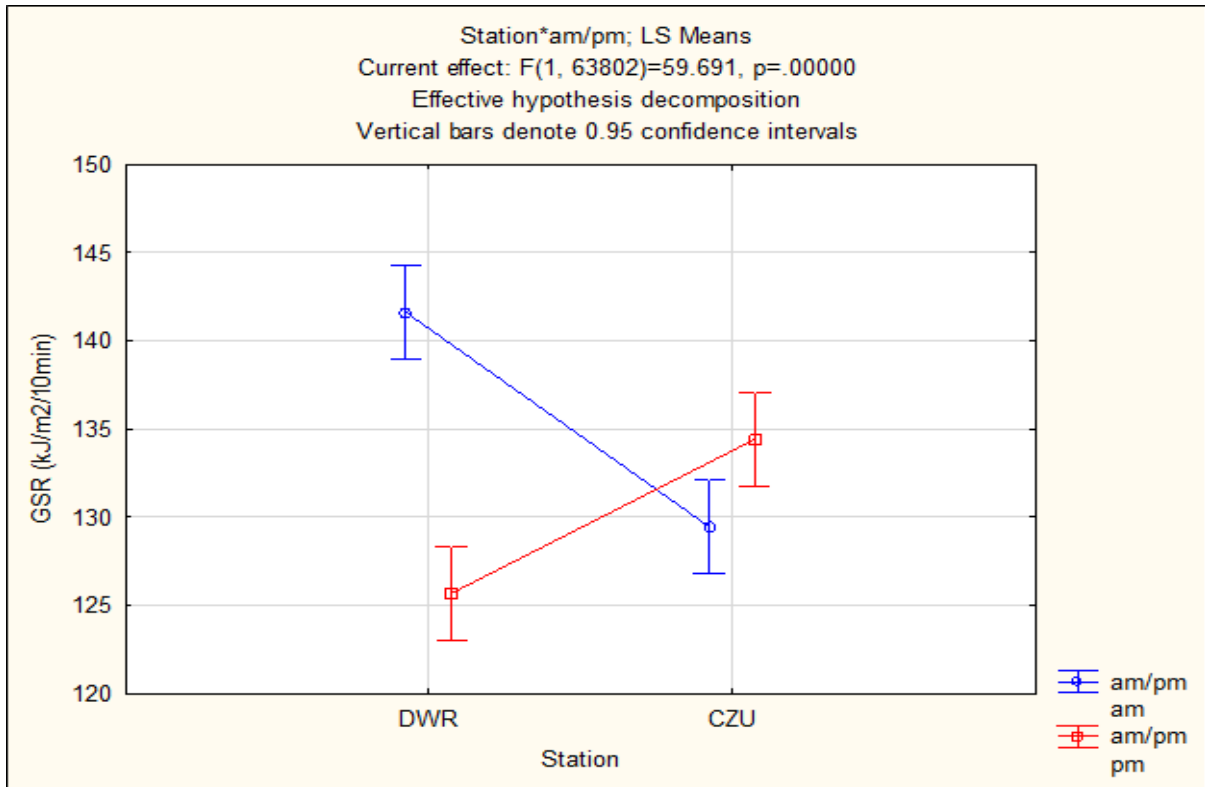


Figure 28 The comparison of global radiation between morning and afternoon.

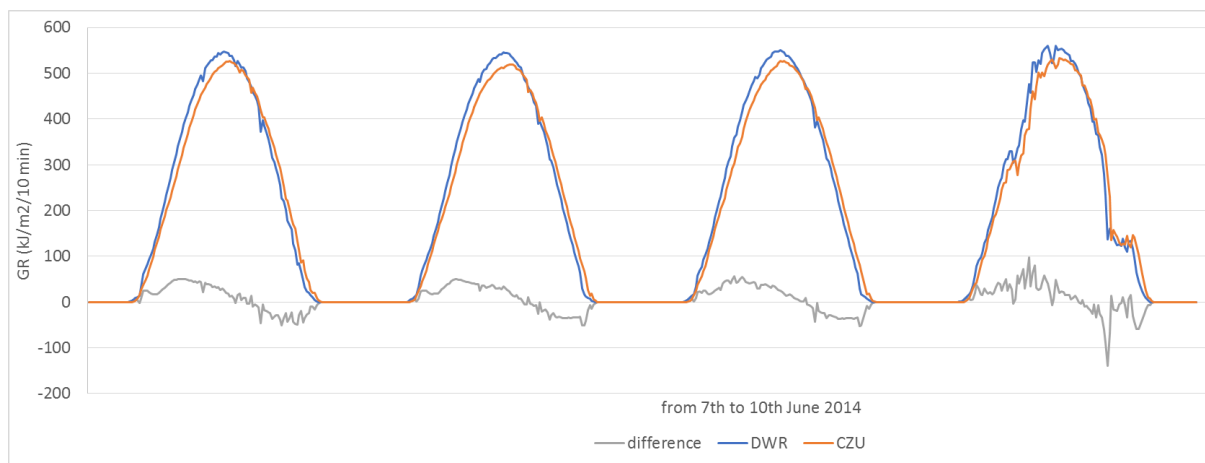
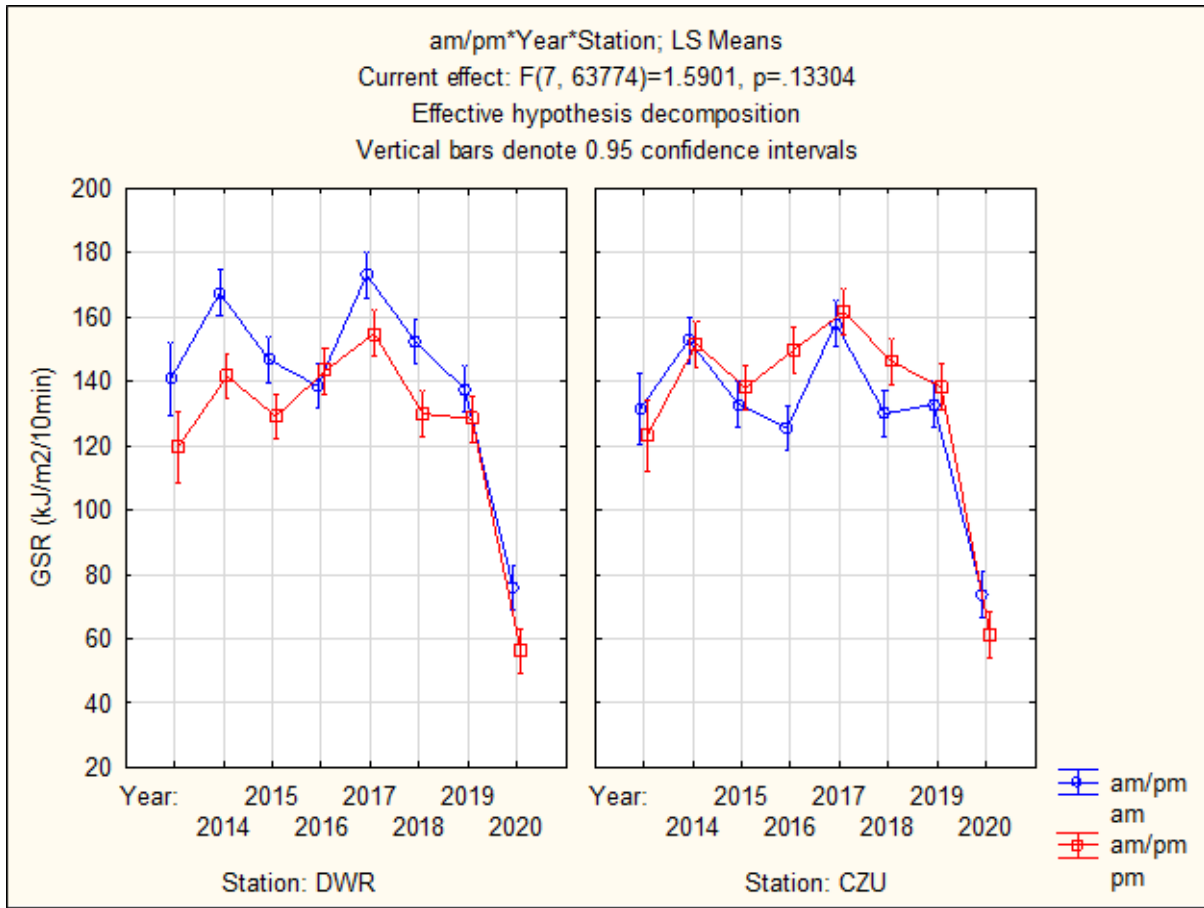


Figure 29 Demonstration of the differences between morning and afternoon values of global radiation in both stations.

Figure 30 indicated that the overall comparison between both meteorological station CZU and DWR were not significantly different ( $P\_Value > 0.05$ ). DWR meteorological station indicated that 2013, 2014, 2015, 2017, 2018, and 2020 were biggest different the amount of solar radiation between daytime and 2016, 2019 showed almost the same of amount of solar radiation between morning (am/pm am) and (am/pm pm).



*Figure 30 Temporal of global radiation in hourly average between CZU and DWR meteorological station*

*Table 11 ANOVA of global radiation in hourly average summary*

Effect	Univariate Tests of Significance for GSR (kJ/m <sup>2</sup> /10min) Sigma-restricted parameterization Effective hypothesis decomposition				
	SS	Degr. of	MS	F	p
Intercept	1.022567E+09	1	1.022567E+09	36071.94	0.000000
am/pm	5.362378E+05	1	5.362378E+05	18.92	0.000014
Year	4.958524E+07	7	7.083606E+06	249.88	0.000000
Station	4.733907E+04	1	4.733907E+04	1.67	0.196273
am/pm*Year	1.372721E+06	7	1.961030E+05	6.92	0.000000
am/pm*Station	1.497485E+06	1	1.497485E+06	52.83	0.000000
Year*Station	8.378002E+04	7	1.196857E+04	0.42	0.889092
am/pm*Year*Station	3.155358E+05	7	4.507654E+04	1.59	0.133037
Error	1.807865E+09	63774	2.834799E+04		

Table 12 demonstrated the summary of statistical information of global radiation in daily average. The result show that both station in 2019 had highest amount of solar radiation 172.40

(KJ.m<sup>-2</sup>.d<sup>-1</sup>), with standard deviation 189.17 (KJ.m<sup>-2</sup>.d<sup>-1</sup>) of CZU and 169.22 (KJ.m<sup>-2</sup>.d<sup>-1</sup>), with standard deviation 190.77 (KJ.m<sup>-2</sup>.d<sup>-1</sup>) of DWR. However, in 2015 showed that the amount of solar radiation had the lowest value in period study from 2014-2020 was about 135.54 (KJ.m<sup>-2</sup>.d<sup>-1</sup>) of CZU , with standard deviation 161.70 (KJ.m<sup>-2</sup>.d<sup>-1</sup>) and 138.19 of DWR, with standard deviation 166.76 (KJ.m<sup>-2</sup>.d<sup>-1</sup>). Therefore, the maximum of solar radiation of CZU and DWR were in 2018 721.30 (KJ.m<sup>-2</sup>.d<sup>-1</sup>), 738. 21 (KJ.m<sup>-2</sup>.d<sup>-1</sup>), respectively. The minimum value of radiation were 0.00 (KJ.m<sup>-2</sup>.d<sup>-1</sup>) of every year of period study from both stations.

*Table 12 Summary of statistic of global radiation hourly average*

Station	Year	mean	stdev	CV	min	max	median	skewness	kurtosis
CZU	2014	152.23	175.60	115.35	0.00	700.80	71.20	0.88	-0.58
	2015	135.54	161.70	119.30	0.00	630.70	60.20	1.02	-0.18
	2016	137.66	163.94	119.09	0.00	644.90	64.40	1.03	-0.13
	2017	159.80	181.74	113.73	0.00	645.70	75.05	0.78	-0.83
	2018	140.17	167.97	119.83	0.00	721.30	60.80	0.99	-0.28
	2019	172.40	189.17	109.73	0.00	591.20	91.90	0.63	-1.15
	2020	117.95	153.87	130.46	0.00	648.10	44.90	1.30	0.58
DWR	2014	154.57	180.69	116.90	0.00	669.10	69.09	0.90	-0.53
	2015	138.19	166.76	120.67	0.00	647.94	59.75	1.04	-0.13
	2016	140.93	169.18	120.05	0.00	635.73	64.85	1.04	-0.14
	2017	164.17	187.70	114.33	0.00	691.50	76.63	0.80	-0.81
	2018	143.27	172.49	120.39	0.00	738.21	61.77	1.00	-0.27
	2019	169.22	190.77	112.74	0.00	612.26	79.80	0.67	-1.09
	2020	115.66	158.19	136.77	0.00	611.65	34.99	1.33	0.58

## 5.10 Wind speed and direction

Figure 31 the graph showed the wind speed and direction in hourly average of CZU meteorological stations categorized at sixteen wind directions and five of wind speed classes based on year record. The value of wind speed and direction derived from anemometer at 10 m above the ground. The wind rose analysis indicated that the prevailing wind direction for 2014 and 2016 were from west to north northwest with wind speed 1 to 5 m/s around 20%. The wind rose in 2017, 2018, 2019 were 30% to 40% about 0 to 5 m/s of wind speed in north northwest. Differently, in 2015 the wind direction indicated that below 20% of 0 to 6 m/s of wind speed flow to west and north northwest. Figure 32 indicated the hourly average of wind speed and direction derived from DWR meteorological station. The result showed that the wind direct in west northwest in the period study from 2014-2020. In 2015 the character of wind direction was separate direction to west and southeast.

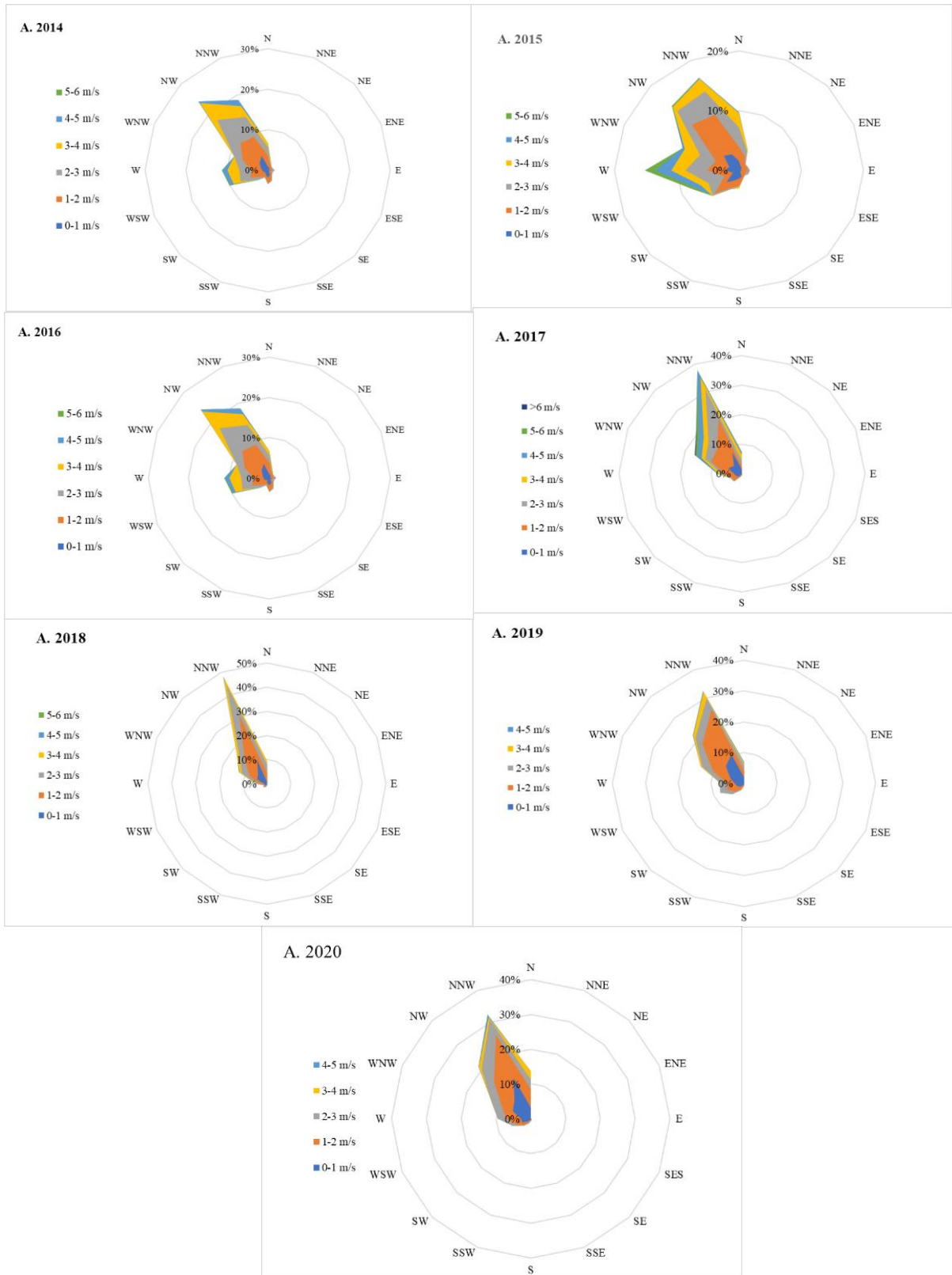


Figure 31 Wind and direction in hourly average of CZU meteorological station during the statistical period of (2014-2020) and colored according to different wind speed

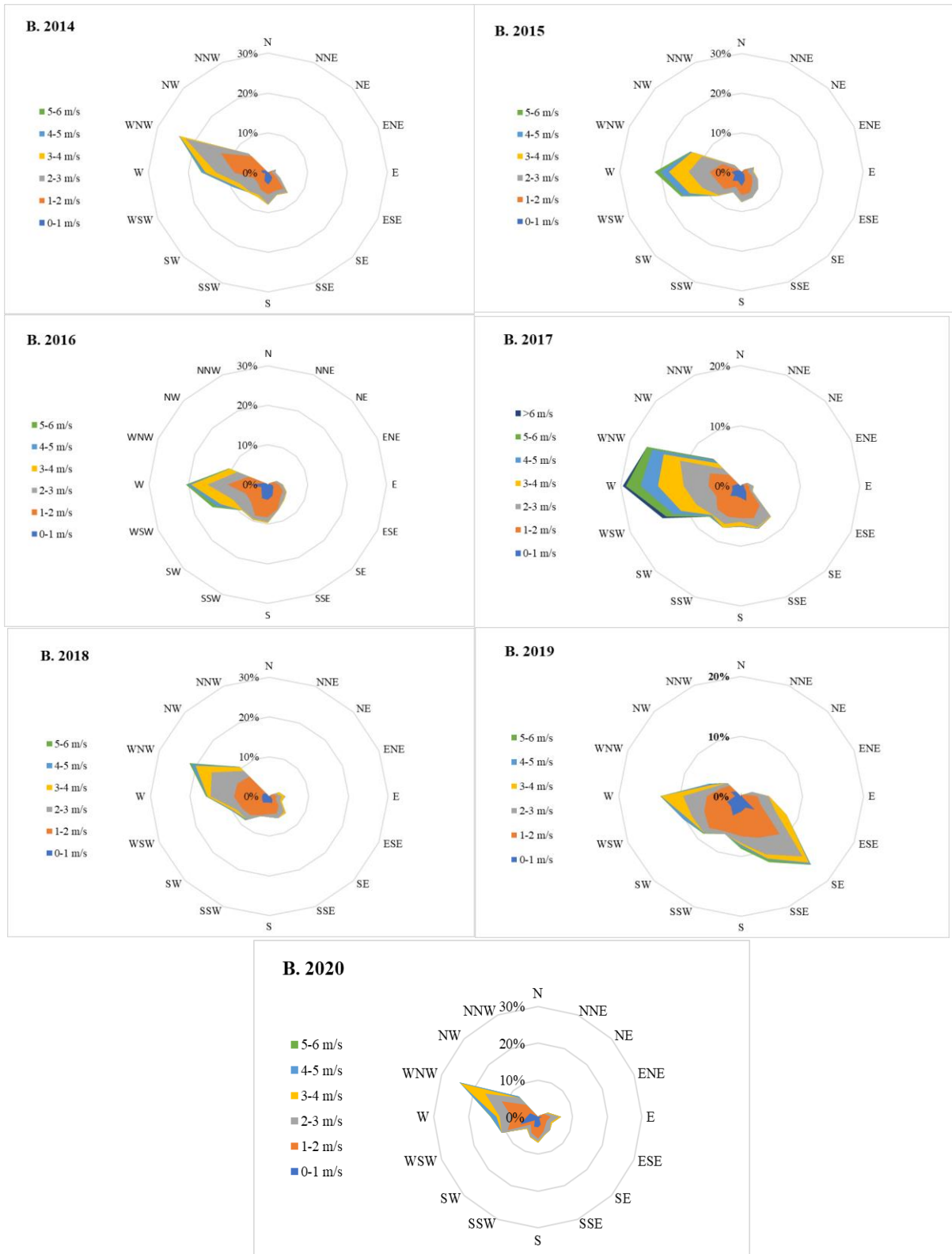


Figure 32 wind rose of Wind speed and direction in hourly average measured at DWR meteorological station and colored according to different wind speed

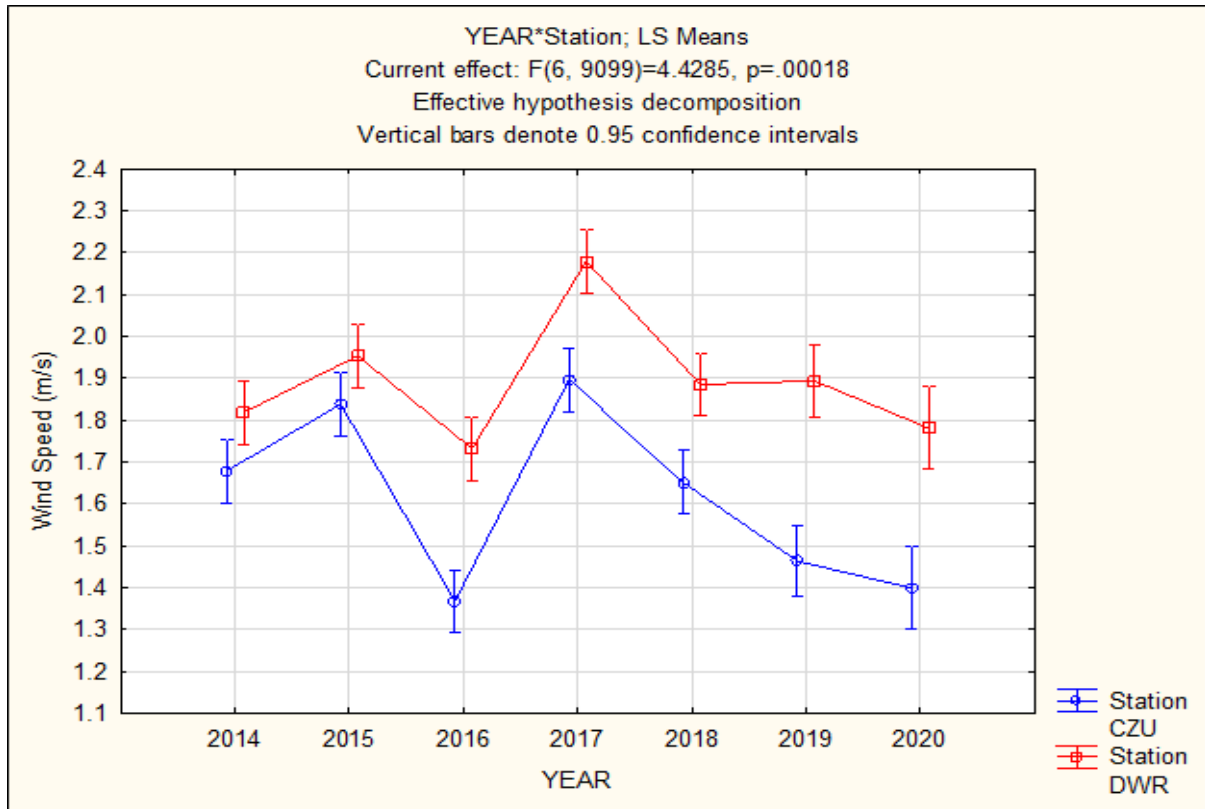


Figure 33 Historical climate record of wind speed hourly average from two different station

Figure 33 above showed the temporal dependence of wind speed from CZU and DWR meteorological station. The result showed that the wind speed of CZU and DWR were statistically significant ( $P_{\text{value}} < 0.05$ ). The study indicated that the speed of wind in 2017 was higher and in 2016 had the lowest of wind speed of both stations. Table 13 illustrated that the temporal dependence of wind speed from 2013-2020 were statistically significant ( $P_{\text{value}} < 0.05$ ). Figure 34 scatter plot of wind speed shows similar trend.

Table 13 ANOVA comparison of wind speed hourly average

Effect	Univariate Tests of Significance for Wind Speed (m/s) Sigma-restricted parameterization Effective hypothesis decomposition				
	SS	Degr. of	MS	F	p
Intercept	26926.96	1	26926.96	25312.13	0.000000
YEAR	231.27	6	38.54	36.23	0.000000
Station	169.90	1	169.90	159.71	0.000000
YEAR*Station	28.27	6	4.71	4.43	0.000177
Error	9679.49	9099	1.06		

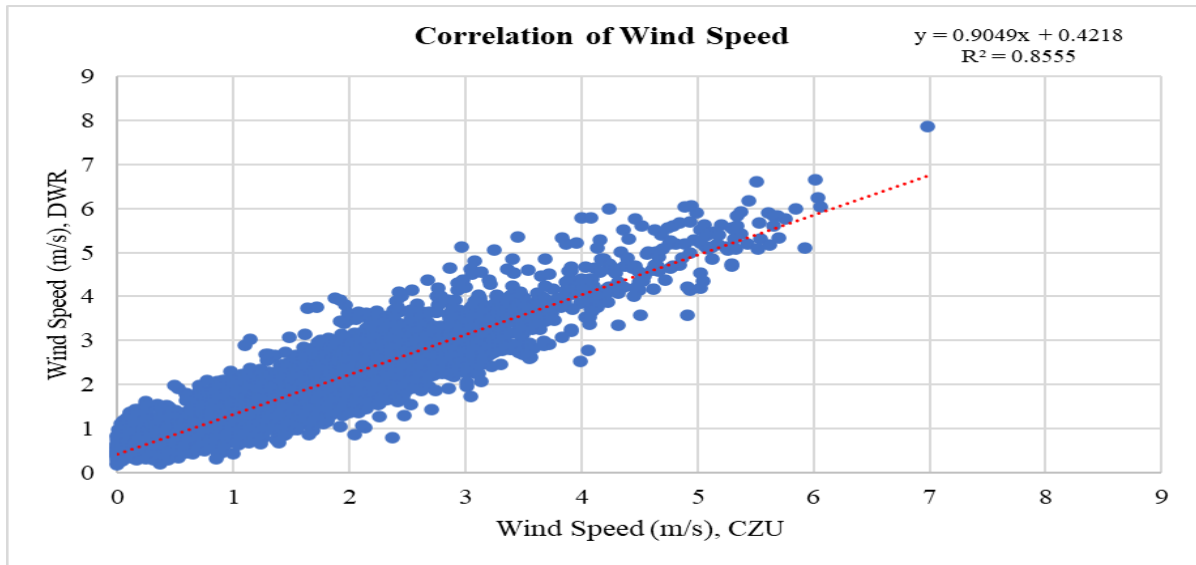


Figure 34 Correlation of wind speed hourly average between CZU and DWR meteorological station

Table 14 indicated the summary of statistical information of wind speed in hourly average of CZU and DWR meteorological station at 10 m above ground. The highest average of daily wind speed from each station was in 2018 313.80 m/s of CZU and at DWR was in 2017 210.34 m/s. However, the lowest of wind speed was in 2015 about 212.40 m/s, with standard deviation 116.07 of CZU and in 2016 about 194.30 m/s, with standard deviation 76.00 m/s of DWR, respectively.

Table 14 Summary of statistic of wind speed hourly average

Station	Year	mean	stdev	CV	min	max	median	skewness	kurtosis
CZU	2014	235.27	110.68	47.05	0.00	360.00	277.50	-0.77	-0.76
	2015	212.40	116.07	54.65	0.00	360.00	255.50	-0.58	-1.10
	2016	352.85	21.60	6.12	0.00	357.00	356.00	-13.80	208.74
	2017	303.78	47.33	15.58	0.00	356.00	316.00	-2.66	11.94
	2018	313.80	43.03	13.71	17.00	355.00	330.00	-2.42	8.66
	2019	297.43	50.83	17.09	7.00	354.00	312.50	-1.89	5.82
	2020	306.58	47.06	15.35	0.00	356.00	319.50	-2.19	8.38
DWR	2014	210.15	73.47	34.96	40.08	327.41	218.99	-0.34	-1.09
	2015	194.30	76.00	39.11	42.51	311.26	205.80	-0.32	-1.19
	2016	193.46	69.54	35.94	41.89	316.76	199.92	-0.32	-1.07
	2017	210.34	69.18	32.89	41.11	322.96	220.81	-0.40	-0.90
	2018	205.13	79.24	38.63	48.45	326.15	221.63	-0.32	-1.26
	2019	172.66	65.14	37.73	31.08	323.36	158.35	0.37	-0.86
	2020	195.88	83.23	42.49	36.40	321.07	201.65	-0.18	-1.44



The variable of hourly average of wind direction of CZU and DWR meteorological station, measured by anemometer at 10 m above ground (Figure 35). The comparison of wind direction of each station was statistically significant ( $P_{\text{value}} < 0.05$ ). Table 15 indicated that the temporal of wind direction was statistically significant ( $P_{\text{value}} < 0.05$ ) in period study from 2014-2020 of both stations.

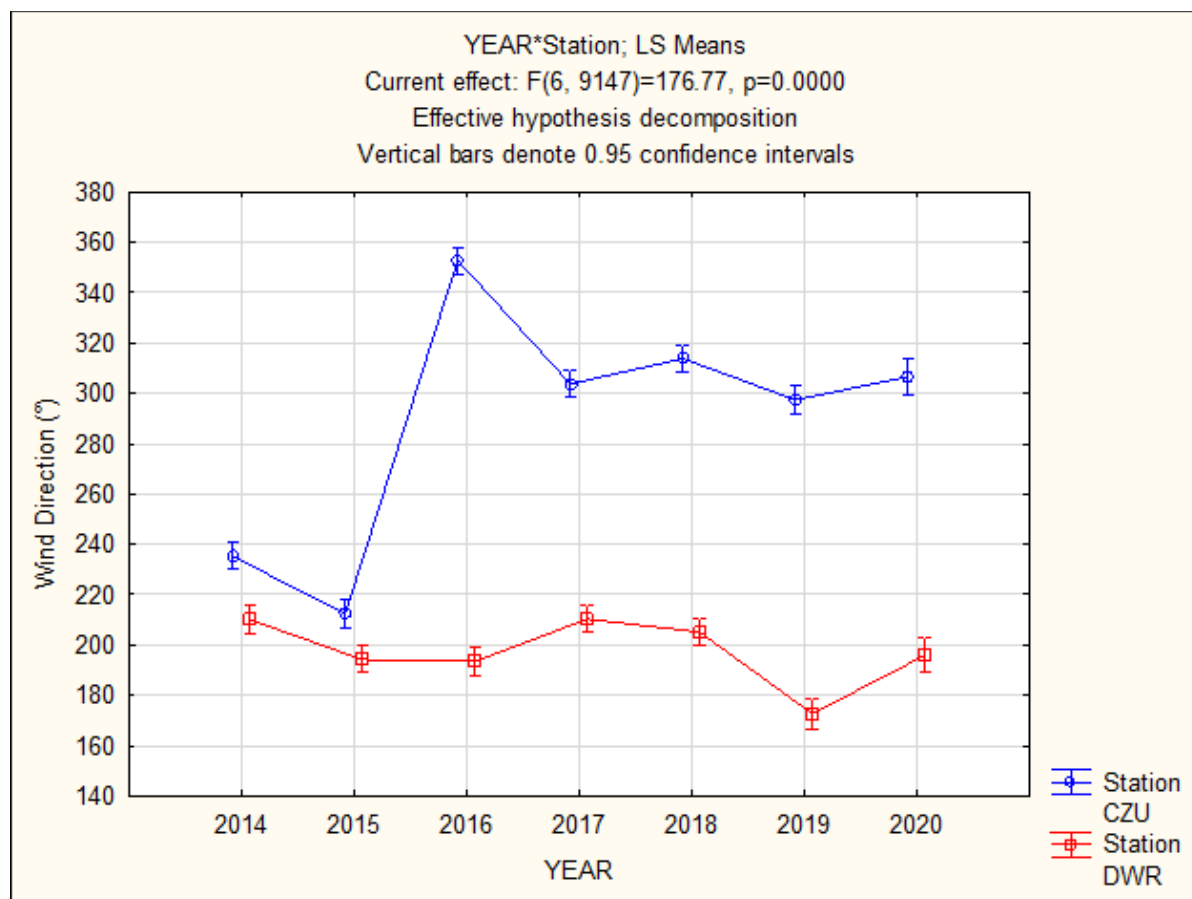


Figure 35 shows the variation of the hourly average wind direction at 2 m above the ground surface.

Table 15 ANOVA of wind direction in hourly average

Effect	Univariate Tests of Significance for Wind Direction (°) Sigma-restricted parameterization Effective hypothesis decomposition				
	SS	Degr. of	MS	F	p
Intercept	524465420	1	524465420	98078.60	0.00
YEAR	4961862	6	826977	154.65	0.00
Station	18549431	1	18549431	3468.87	0.00
YEAR*Station	5671567	6	945261	176.77	0.00
Error	48912662	9147	5347		

Table 16 Overall results of ANOVA for each variable

Meteorological variables	CZU	DWR	year	station	year*station	am/pm*station
Air Temperature at 2 m		*	0.000	0.000008	0.999993	
Air Temperature diurnal		*	0.000000	0.011011	0.999976	
Air humidity in 2 m	*		0	0	0.379092	
Air humidity diurnal		*	0.000000	0.000725	0.999933	
Temperature Extreme		*	0	0.300569	1	
Global Radiation		*	not significant			
GR am		*	0	0.196273	0.889092	0
GR pm	*		0	0.196273	0.889092	0
Wind Speed		*	0	0	0.000177	
Wind Direction	*		0	0	0	
Daily Totals of Precipitation	*		0.005061	0.222691	0.998841	

Note: \* indicating higher value

## **6 Discussion**

### **6.4 Effect of air humidity**

Humidity in air is an important variable used in different industries such as chemical, food, agriculture, climate. However, there are some studies that indicated the climate record of air humidity measurement. Duchan et al. (2020) has been addressing that extreme flooding affected namely western regions of the Czech Republic, Bohemian part. Flooding event in 2013 was reported the heaviest rainfall event in the region 9 years after the 2002. May 2013 had been one of the three wettest months in the last century. On May 30 to June 1 upper areas of the Elbe and Vltava river basins experienced rainfall intensity varying from 150 to 200 mm, locally reaching even 250 mm, which in just a few days was the equivalent normally occurring over two and half months on average. In the results section, it was found that the amount of air humidity is highest in 2013 and lowest in 2019 (Fig 19) of both CZU and DWR station based on Dunn et al. (2015) & Hersbach et al. (2020) the heat event in 2019 causing the amount of air humidity in environment becoming lower than other period study (2013-2020). To summarize the results, it can be observed that the amount of humidity in Czech Republic from stations were accurate with other stations and reports based on two different events: flooding in 2013 and heat wave event in 2019. The statistically significant differences between the DWR and CZU stations might be caused by lower air movement among the buildings at CZU station.

### **6.5 Effect of air temperature, and temperature extreme**

Temperature is known as the feature of cool and hot of the air surrounding the globe. However, the indirect effect of air temperature is solar radiation. There are several studies that reported that air temperature in 2019 was known as the second-warmest year.

Based on the analysis of temporal climate records obtained from CZU and DWR meteorological stations, it was shown that even though weather stations represent different microclimatic conditions, no substantial differences occurred in the results of these two stations. Higher values of the amplitude of the air temperature above the line (Figure 20) document that at the DWR station, which is located in the open space of the CZU experimental plot, the surface is a more significant element in air heating during the day and radiation at night. But statistically significant by year in period study from 2013-2020. In 2019 had the highest of air temperature of both meteorological stations due to Dunn et al. (2015) & Hersbach et al. (2020) the number of days is frequently high in warm days over European countries and part of Asia as well corresponding with the heat wave event in 2019 mainly around in March, June, July, which

should result in an increase in the rate of evaporation from the surface water the heat wave event in Europe. These results confirm what we found at the site that the temperature extreme in 2019 was about 37.30°C from CZU and 37.10°C DWR was showed above normal average. *Annual report of CHMI (2019)* has reported that the year 2019 in the Czech Republic was exceptionally above normal, the average annual temperature of 9.5 ° C was 1.6 ° C higher than normal 1981-2010. The most significant positive deviation from normal (+ 4.9 ° C) was recorded in June, and this month was assessed as extremely above normal. On the contrary, May was strongly below normal with a deviation -2.3 ° C from normal 2019 is thus the second warmest year recorded in the period since 1961. Higher average annual air temperature was recorded only in the previous year (2018), namely 9.6 ° C. The deviation of the average monthly temperature from the normal 1981–2010 was for all months of 2019, except May, positive. (<https://www.chmi.cz/historicka-data/pocasi/zakladni-informace?l=en>) has reported that for Prague and Middle Bohemia the long-term average temperature (considered between years 1981 and 2010) in June is 16.5°C, and long-term average precipitation is 70 mm. It was further investigated numerically by Hájková et al. (2018) has reported that in the period of 1971–2015 showed that areas of some part of the south Moravia in which surroundings of Brno city and Prague city and Poohří river basin shifted gradually to sub-humid climate zone as before as wet region.

## **6.6 Effect of daily precipitation totals**

Precipitation as the source of water on the planet for the natural environment and human activity, is among most frequently studied elements of climatology. However, some natural hazard may result from the coincidences of anomalies of different weather variables. Precipitation is one of the most variable meteorological elements. They have a strong local character, where a number of factors are manifested (obstacles, wind direction, precipitation intensity, particle size and more). In a previous numerical study by Tichavský et al. (2021) the most frequent floods occurred from May to July. In addition, in ten event years it was possible to identify multiple flood events: for example, May and July–August floods in 2010, 2014, and 2016. The monthly precipitation showed the strongest, but still weak, correlation with indices of Scandinavian climate oscillation during summer months ( $R_s = 0.23\text{--}0.42$ ;  $p < 0.00$ ), suggesting the influence of a blocking anticyclone over Scandinavia and wet air propagation to central Europe. Mekonnen et al., (2015) has reported that there is a relationship between logarithmic wind profile and its effect on the catch ratio (CR) of the two gauges, was used to determine the daily basis and the intensity of rainfall the effect of wind speed. An increasing

number of studies addressing regional flood chronologies based on Rulfová et al. (2021) the analyzed for the period 1982–2016 that the maximum of monthly convective precipitation from stations 52 mm occurs in July. In contrast, the monthly average fall almost to zero in February. Monthly stratiform precipitation amounts are nearly constant during the year and range from 33 to 48 mm with SD around 20 mm. The annual cycle of total precipitation is composed of convective and stratiform precipitation, with mean July value of 96 mm and mean February value of 39 mm. According to analyzed obtained from CZU and DWR meteorological station show that the maximum of daily precipitation was 72 mm in 2013 of CZU and 38.70 mm in of DWR meteorological station in which during at year the flooding event was occurrence. Brázdil et al. (2021) has reported Analysis of series of monthly, seasonal, and annual precipitation totals revealed relatively stable fluctuations, while linear trends remained largely insignificant. that significant interannual variability on a timescale of 4–8-years in seasonal and annual series. The minimum in annual variation tended to appear in February (also in January and, at higher altitudes, in April) with the maximum favoring July (but also June and August).

In terms of precipitation, the year 2019 was normal in the Czech Republic; the average annual total precipitation of 634 mm represents 92% of the 1981–2010 normal. During the year, 7 months were assessed as precipitation normal. It was below normal in terms of precipitation April (60% of normal), June (67% of normal) and July (66% of normal). They were above normal in terms of precipitation evaluated months January (148% of normal) and May (132% of normal). The spatial distribution of the annual total precipitation was uneven. An average of 601 mm of precipitation fell on the territory of Bohemia (88% of normal), while on the territory of Moravia and Silesia it was 701 mm (102% of normal) (*Annual report of CHMI, 2019*).

## **6.7 The effect of global radiation based on direction sunlight**

Global radiation is made up of electromagnetic waves which travel from the sun to the earth with the form of the speed light. There are several studies that reported the amount of global radiation could reduce based the urban development while some studies found opposite results. Their findings were strongly clarified by a measurement made by Chalkias et al. (2013) The result of this procedure is a map illustrating the sections of the road where direct sunlight includes a serious amount of risk for the drivers. Zhao et al. (2016) has reported that the rugged surface of an urban area due to developing buildings can interact with solar radiation and affect both the magnitude and spatiotemporal distribution of surface solar fluxes. However, the study showed at noontime, buildings generally receive more solar energy than a flat surface area due

to a larger area facing the sun, whereas negative result in the early morning and late afternoon are primarily induced by larger shading areas.

This reveals the similarity (Fig 28) the amount of solar radiation of CZU station at noon time is higher than the morning due to higher building than DWR station in which located in open field. The result indicated that urban and open filed meteorological station at CZU and DWR record of the study their impacts on surface radiation of daytime. The differences between the morning and afternoon values at the stations are determined primarily by the movement of the Sun on the horizon and the variability of the direct and diffuse components of global radiation. They are clear in Figure 29, where there are greater differences in daily running in the afternoon at stations. At CZU where known as the urban station showed that were statistically different at morning and afternoon of solar radiation the same as the climate data from DWR based on observation (Fig 30) On other hand, the amount of solar radiation between CZU and DWR indicated that significantly different.

It was similarly to Takebayashi et al. (2017) showed that in open space and green garden, generally received solar radiation by the buildings in which located behind the rather than by the trees themselves. Solar radiation shielding by trees is necessary in the range of more than 10 m from the south side of the buildings and more than 6 m from the west or east sides of the buildings. So, the amount of solar radiation had affected by the building and daytime due to tall building receiving the solar directly from the Sun and causing the meteorological area cover with shadow of building (Fig 29) as the result DWR received higher solar radiation than CZU.

## **6.8 Effect of wind speed and direction according to urban development**

Wind speed prediction could play an important role in improving the performance of wind turbine control and condition monitoring. The course of the wind direction above the mean roof level of Freiburg exhibits two major directions: between  $240^{\circ}$  and  $330^{\circ}$  during the daylight hours and around  $120^{\circ}$  in the night from 9 pm to 6am CET. (Matzarakis & Mayer, 2014). Bornstein et al. (1977) Wind speeds along a streamflow line through New York City are found to be decreased below (increased above) those at sites outside of the city during periods with regional wind speeds above (below) about 4 m/s. The decrease is attributed to increased values of the surface roughness parameter in the city, as compared to values in nearby non-urban regions. The increase is associated with accelerations produced by a well-developed urban heat island. As the result of study had showed the wind direction in CZU was different than DWR meteorological. The comparison between CZU and DWR was statistically significant due CZU station had been build the new infrastructure around the station. So, It can be measured that the wind speed in urban area are higher than open field. Huifen et al. (2014)

has described the building (height-to-width) aspect ratio is one of the most important elements that determined the flow field inside a street canyon. Droste et al. (2018) have also found that for certain atmospheric conditions the mean wind speed in a city can surprisingly be higher than its rural area, despite the higher roughness of city. It was surface roughness and the ageostrophic wind, between city and countryside and indicated that low-rise buildings (up to 12 m) and a moderate geostrophic wind ( $\sim 5\text{ms}^{-1}$ ).

## **6.9 Effect of weather viable between urban and open field meteorological station**

The effect of climate condition between open field and urban meteorological station had been some different weather condition. Therefore, understanding the mechanisms that control urban climates has substantial societal importance to a variety of sectors, including public health and energy management. Fortuniak, (2004) has reported that urban–rural contrasts of such parameters as air temperature, relative humidity, water vapour pressure and wind speed. weather conditions the highest temperature differences between the urban and rural station exceeds 8 °C. Relative humidity was lower in the town, sometimes by more than 40%. Water vapour pressure differences can be either positive (up to 5 hPa) or negative (up to 4 hPa). Wind speed at the urban station is on average lower by about 34% in night and 39% during daytime.

The pattern of the incoming short-wave radiation reflects the cloudless conditions. Peak 10-min mean air temperature reached 35 °C. The patterns for vapour pressure and relative humidity show that the humidity conditions were not in a stress range for people (Matzarakis & Mayer, 2014) In terms of education, the students in Freiburg are in close contact with the actual meteorological situation and are asked to discuss and explain weather conditions or specific phenomena like strong change of wind direction or air temperature drops from the starting semester.

## 7 Conclusion

Urban development and its impact on microclimate need to be investigated in order to better understand and quantify the effect on meteorological variables. This study evaluates the comparison of rural and urban meteorological station in terms of land surface. According to the results, meteorological station is significantly different in various meteorological variables in each year will be considered separately, there will be difference between stations in many parameters (Table 16). Weather variables such as air humidity, temperature, pressure, precipitation, and solar radiation are significantly different ( $P\_value < 0.05$ ) either wind speed and direction are significantly different both by year\*station corresponding to the barrier of the building in the urban meteorological cause the wind speed a bit lower than open field meteorological station. However, the historical records of both stations in study period 2013-2020 were significantly different. Furthermore, in 2019 is known as the second warmest year of the record because of the heat wave even over the central Europe. On the other hand, in 2013 is very high in precipitation and air humidity due to rain intensity and flooding event in European countries. The comparison between two different meteorological station at Czech University of Life Sciences Prague is based on meteorological station locality, urban and rural area. However, urban development main function of influencing on future changing of infrastructure and global climate change. To sum up, during the period of observation, compared to the CZU meteorological station representing the urban microclimate, the DWR meteorological station representing the rural microclimatic conditions showed slightly higher average air temperature, lower air humidity, higher diurnal differences in both temperature and humidity, mostly lower precipitation in correspondence with higher wind speed and higher global radiation in the morning while lower in the afternoon, thus the hypothesis was confirmed and the objectives of the thesis were fulfilled.



## Bibliography

- Allen, R. G., Pereira, L. S., Raes, D., & Smith, M. (1998). Crop evapotranspiration guidelines for computing crop water requirements. In *FAO Irrigation & drainage Paper 56*. FAO, Food and Agriculture Organization of the United Nations, Roma.
- An, N., Hemmati, S., & Cui, Y. J. (2017). Assessment of the methods for determining net radiation at different timescales of meteorological variables. *Journal of Rock Mechanics and Geotechnical Engineering*, 9(2), 239–246. <https://doi.org/10.1016/j.jrmge.2016.10.004>
- Bai, Y., Meng, X., Guo, H., Liu, D., Jia, Y., & Cui, P. (2021). Design and validation of an adaptive low-power detection algorithm for three-cup anemometer. *Measurement: Journal of the International Measurement Confederation*, 172(December 2020), 108887. <https://doi.org/10.1016/j.measurement.2020.108887>
- Baird, C., Cann., M. (2008). *Environmental Chemistry*. New York: Clancy Marshall.
- Bartoszek, K., & Matuszko, D. (2021). The influence of atmospheric circulation over Central Europe on the long-term variability of sunshine duration and air temperature in Poland. *Atmospheric Research*, 251(October 2020), 105427. <https://doi.org/10.1016/j.atmosres.2020.105427>
- Blunden, J., Arndt, D. S., Bissolli, P., Diamond, H. J., Druckenmiller, M. L., Dunn, R. J. H., Ganter, C., Gobron, N., Lumpkin, R., Richter-Menge, J. A., Li, T., Mekonnen, A., Sánchez-Lugo, A., Scambos, T. A., Schreck, C. J., Stammerjohn, S., Stanitski, D. M., Willett, K. M., Andersen, A., & Rosen, R. (2020). State of the climate in 2019. *Bulletin of the American Meteorological Society*, 101(8), S1–S8. [https://doi.org/10.1175/2020BAMSSTATEOFTHECLIMATE\\_INTRO.1](https://doi.org/10.1175/2020BAMSSTATEOFTHECLIMATE_INTRO.1)
- Boilley, A., & Wald, L. (2015). Comparison between meteorological re-analyses from ERA-Interim and MERRA and measurements of daily solar irradiation at surface. *Renewable Energy*, 75(March), 135–143. <https://doi.org/10.1016/j.renene.2014.09.042>
- Bornstein, R. D., & Johnson, D. S. (1977). Urban-rural wind velocity differences. *Atmospheric Environment* (1967), 11(7), 597–604. doi:10.1016/0004-6981(77)90112-3

- Brázdil, R., Zahradníček, P., Dobrovolný, P., Štěpánek, P., & Trnka, M. (2021). Observed changes in precipitation during recent warming: The Czech Republic, 1961–2019. *International Journal of Climatology*, *October 2020*, 1–22. <https://doi.org/10.1002/joc.7048>
- CAMPBELL SCIENTIFIC, INC. UK (2001). RPT410F Barometric Pressure Sensor. *44*(October), 601141.
- CAMPBELL SCIENTIFIC, INC. UK (2002). *Model Hmp45C Temperature and Relative Humidity Probe. c*, 16.
- Cao, J., Zhou, W., Zheng, Z., Ren, T., & Wang, W. (2021). Within-city spatial and temporal heterogeneity of air temperature and its relationship with land surface temperature. *Landscape and Urban Planning*, *206*(October 2020), 103979. <https://doi.org/10.1016/j.landurbplan.2020.103979>
- Carpio, M., González, Á., González, M., & Verichev, K. (2020). Influence of pavements on the urban heat island phenomenon: A scientific evolution analysis. *Energy and Buildings*, *226*, 110379. <https://doi.org/10.1016/j.enbuild.2020.110379>
- Chalkias, C., Faka, A., & Kalogeropoulos, K. (2013). Assessment of the Direct Sun-Light on Rural Road Network through Solar Radiation Analysis Using GIS. *Open Journal of Applied Sciences*, *03*(02), 224–231. <https://doi.org/10.4236/ojapps.2013.32030>
- Cianci, J., Boyle, A. G., Stefanovski, D., & Biddle, A. S. (2021). Lack of Association Between Barometric Pressure and Incidence of Colic in Equine Academic Ambulatory Practice. *Journal of Equine Veterinary Science*, *97*, 103342. <https://doi.org/10.1016/j.jevs.2020.103342>
- Doležal, F., Hernandez-Gomis, R., Matula, S., Gulamov, M., Miháliková, M., & Khodjaev, S. (2018). Actual Evapotranspiration of Unirrigated Grass in a Smart Field Lysimeter. *Vadose Zone Journal*, *17*(1), 170173. <https://doi.org/10.2136/vzj2017.09.0173>
- Doležal, F., Matula, S., & Moreira Barradas, J. M. (2015). Rapid percolation of water through soil macropores affects reading and calibration of large, encapsulated TDR sensors. *Soil and Water Research*, *10*(3), 155–163. <https://doi.org/10.17221/177/2014-SWR>

- Droste, A. M., Steeneveld, G. J., & Holtslag, A. A. M. (2018). Introducing the urban wind island effect. *Environmental Research Letters*, 13(9). <https://doi.org/10.1088/1748-9326/aad8ef>
- Duchan, D., Dráb, A., & Říha, J. (2020). *Flood Protection in the Czech Republic. August 2019*, 333–363. [https://doi.org/10.1007/978-3-030-18359-2\\_14](https://doi.org/10.1007/978-3-030-18359-2_14)
- Fortuniak, K., Kłysik, K., & Wibig, J. (2006). Urban - Rural contrasts of meteorological parameters in Łódź. *Theoretical and Applied Climatology*, 84(1–3), 91–101. <https://doi.org/10.1007/s00704-005-0147-y>
- Fu, G., Charles, S. P., & Yu, J. (2009). A critical overview of pan evaporation trends over the last 50 years. *Climatic Change*, 97(1), 193–214. <https://doi.org/10.1007/s10584-009-9579-1>
- Giannopoulou, K., Santamouris, M., Livada, I., Georgakis, C., & Caouris, Y. (2010). The impact of canyon geometry on intra Urban and Urban: Suburban night temperature differences under warm weather conditions. *Pure and Applied Geophysics*, 167(11), 1433–1449. <https://doi.org/10.1007/s00024-010-0099-8>
- Givoni, B. (1969). *Man: climate, and architecture: Building research station Technion, Israel Institute of Technology*, pp. 1-18.
- Hájková, L., Bartošová, L., & Kožnarová, V. (2018). Evaluation of aridity index in the Czech Republic within 1961 - 2015. *Acta Universitatis Agriculturae et Silviculturae Mendelianae Brunensis*, 66(5), 1111–1118. <https://doi.org/10.11118/actaun201866051111>
- Harris, I., Jones, P. D., Osborn, T. J., & Lister, D. H. (2014). Updated high-resolution grids of monthly climatic observations - the CRU TS3.10 Dataset. *International Journal of Climatology*, 34(3), 623–642. <https://doi.org/10.1002/joc.3711>
- Hersbach, H., Bell, B., Berrisford, P., Hirahara, S., Horányi, A., Muñoz-Sabater, J., Nicolas, J., Peubey, C., Radu, R., Schepers, D., Simmons, A., Soci, C., Abdalla, S., Abellan, X., Balsamo, G., Bechtold, P., Biavati, G., Bidlot, J., Bonavita, M., ... Thépaut, J. N. (2020). The ERA5 global reanalysis. *Quarterly Journal of the Royal Meteorological Society*, 146(730), 1999–2049. <https://doi.org/10.1002/qj.3803>

- Hubbard, K. G., & Hollinger, S. E. (2015). *Standard Meteorological Measurements*. 1–30. <https://doi.org/10.2134/agronmonogr47.c1>
- Huifen, Z., Fuhua, Y., & Qian, Z. (2014). Research on the Impact of Wind Angles on the Residential Building Energy Consumption. *Mathematical Problems in Engineering*, 2014. <https://doi.org/10.1155/2014/794650>
- Kanniah, K. D., Beringer, J., North, P., & Hutley, L. (2012). Control of atmospheric particles on diffuse radiation and terrestrial plant productivity: A review. *Progress in Physical Geography*, 36(2), 209–237. <https://doi.org/10.1177/0309133311434244>
- Libralato, M., Murano, G., de Angelis, A., Saro, O., & Corrado, V. (2020). Influence of the meteorological record length on the generation of representative weather files. *Energies*, 13(8), 1–19. <https://doi.org/10.3390/en13082103>
- Lin, H., Liu, F., Dai, Y., & Mumtaz, F. (2020). Relative humidity sensor based on FISM-SMS fiber structure coated with PVA film. *Optik*, 207(January), 164320. <https://doi.org/10.1016/j.ijleo.2020.164320>
- Matzarakis, A., & Mayer, H. (2008). Importance of urban meteorological stations - the example of Freiburg , Germany. *Ber Meteorol Inst Univ Freiburg*, 17(May 2014), 119–128.
- Mekonnen, G. B., Matula, S., Doležal, F., & Fišák, J. (2015). Adjustment to rainfall measurement undercatch with a tipping-bucket rain gauge using ground-level manual gauges. *Meteorology and Atmospheric Physics*, 127(3), 241–256. <https://doi.org/10.1007/s00703-014-0355-z>
- Middleton, W.E. Knowles. 1969. *Invention of the meteorological instruments*. Johns Hopkins Press, Baltimore, MD.
- Mozny, M., Trnka, M., Vlach, V., Vizina, A., Potopova, V., Zahradnicek, P., Stepanek, P., Hajkova, L., Staponites, L., & Zalud, Z. (2020). Past (1971–2018) and future (2021–2100) pan evaporation rates in the Czech Republic. *Journal of Hydrology*, 590(2020), 125390. <https://doi.org/10.1016/j.jhydrol.2020.125390>

- Pearce, J. A., Valvano, J. W., & Emelianov, S. (2011). Temperature measurements. *Optical-Thermal Response of Laser-Irradiated Tissue*, 399–453. [https://doi.org/10.1007/978-90-481-8831-4\\_11](https://doi.org/10.1007/978-90-481-8831-4_11)
- Phillips, R. C., Saylor, J. R., Kaye, N. B., & Gibert, J. M. (2016). A multi-lake study of seasonal variation in lake surface evaporation using MODIS satellite-derived surface temperature. *Limnology*, 17(3), 273–289. <https://doi.org/10.1007/s10201-016-0481-z>
- Prado, S. G., Collazo, J. A., Marand, M. H., & Irwin, R. E. (2021). The influence of floral resources and microclimate on pollinator visitation in an agro-ecosystem. *Agriculture, Ecosystems and Environment*, 307, 107196. <https://doi.org/10.1016/j.agee.2020.107196>
- Robert E. Gabler, James F. Petersen, L. M. T. (2008). Atmospheric pressure, winds, and circulation patterns. *Weather*, 113–137.
- Rodrigo, F. S. (2012). Completing the early instrumental weather record from Cádiz (Southern Spain): New data from 1799 to 1803. *Climatic Change*, 111(3), 697–704. <https://doi.org/10.1007/s10584-011-0174-x>
- RPT410F Barometric Pressure Sensor*. (2001). 44(October), 601141.
- Rulfová, Z., Beranová, R., & Plavcová, E. (2021). Compound Temperature and Precipitation Events in the Czech Republic: Differences of Stratiform versus Convective Precipitation in Station and Reanalysis Data. *Atmosphere*, 12(1), 87. <https://doi.org/10.3390/atmos12010087>
- Rutledge, K., Ramroop, T., Boudreau, D., Mcdaniel. M., Teng, S., Sprout, E., Costa, H., Hall, H., Hunt, J. (2011). Atmospheric Pressure. National Geographic Society. <https://www.nationalgeographic.org/encyclopedia/atmospheric-pressure/>
- Schmitz, U., & Dericks, G. (2010). Influence of solar radiation and soil moisture on growth and yield of Chinook wheat. Soil and moisture demand (*Flora*), 205(11), 772–776. <http://dx.doi.org/10.1016/j.flora.2009.12.037>

- Schober, P., & Schwarte, L. A. (2018). Correlation coefficients: Appropriate use and interpretation. *Anesthesia and Analgesia*, *126*(5), 1763–1768. <https://doi.org/10.1213/ANE.0000000000002864>
- Selase, A. E., Eunice, D., Agyimpomaa, E., Selasi, D. D., Melody, D., & Hakii, N. (2015). Precipitation and Rainfall Types with Their Characteristic Features. *Journal of Natural Sciences Research*, *5*(20), 2225–2921.
- Serrano-Notivoli, R., Martín-Vide, J., Saz, M. A., Longares, L. A., Beguería, S., Sarricolea, P., Meseguer-Ruiz, O., & de Luis, M. (2018). Spatio-temporal variability of daily precipitation concentration in Spain based on a high-resolution gridded data set. *International Journal of Climatology*, *38*(2018), e518–e530. <https://doi.org/10.1002/joc.5387>
- Shao, Q., Sun, C., Liu, J., He, J., Kuang, W., & Tao, F. (2011). Impact of urban expansion on meteorological observation data and overestimation to regional air temperature in China. *Journal of Geographical Sciences*, *21*(6), 994–1006. <https://doi.org/10.1007/s11442-011-0895-9>
- Shi, Y., Song, L., Xia, Z., Lin, Y., Myneni, R. B., Choi, S., Wang, L., Ni, X., Lao, C., & Yang, F. (2015). Mapping annual precipitation across Mainland China in the period 2001-2010 from TRMM3B43 product using spatial downscaling approach. *Remote Sensing*, *7*(5), 5849–5878. <https://doi.org/10.3390/rs70505849>
- Swarno, H. A., Zaki, S. A., Hagishima, A., & Yusup, Y. (2020). Characteristics of wind speed during rainfall event in the tropical urban city. *Urban Climate*, *32*(January), 100620. <https://doi.org/10.1016/j.uclim.2020.100620>
- Takebayashi, H., Kasahara, M., Tanabe, S., & Kouyama, M. (2017). Analysis of solar radiation shading effects by trees in the open space around buildings. *Sustainability (Switzerland)*, *9*(8), 1–9. <https://doi.org/10.3390/su9081398>
- Tichavský, R., Fabiánová, A., & Tolasz, R. (2021). Intra-annual dendrogeomorphic dating and climate linkages of flood events in headwaters of central Europe. *Science of the Total Environment*, *763*. <https://doi.org/10.1016/j.scitotenv.2020.142953>

- Valeriánová, A., Crhová, L., Holtanová, E., Kašpar, M., Müller, M., & Pecho, J. (2017). High temperature extremes in the Czech Republic 1961–2010 and their synoptic variants. *Theoretical and Applied Climatology*, 127(1–2), 17–29. <https://doi.org/10.1007/s00704-015-1614-8>
- Van Kooten G.C. (2013) Weather and the Instrumental Record. In: Climate Change, Climate Science and Economics. Springer, Dordrecht. [https://doi.org/10.1007/978-94-007-4988-7\\_2](https://doi.org/10.1007/978-94-007-4988-7_2)
- Výroční zpráva ČHMÚ 2019 Pozorovací síť.* (2019).
- Wang, J. A., Hutyrá, L. R., Li, D., & Friedl, M. A. (2017). Gradients of atmospheric temperature and humidity controlled by local urban land-use intensity in Boston. *Journal of Applied Meteorology and Climatology*, 56(4), 817–831. <https://doi.org/10.1175/JAMC-D-16-0325.1>
- Wang, Y., Guan, J., Zhang, X., Du, P., Zhang, L., & Luo, M. (2019). Characterizing the properties of daily precipitation concentration in Amur River Basin of northeast China. *E3S Web of Conferences*, 117. <https://doi.org/10.1051/e3sconf/201911700003>
- Wang, Z., Ding, Y., Zhang, Q., & Song, Y. (2012). Changing trends of daily temperature extremes with different intensities in china. *Acta Meteorologica Sinica*, 26(4), 399–409. <https://doi.org/10.1007/s13351-012-0401-z>
- Wisniak, J. (2000). The Thermometer-From The Feeling To The Instrument. *The Chemical Educator*, 5(2), 88–91. <https://doi.org/10.1007/s00897990371a>
- WMO. (2010). Chapter 5 Measurement of Atmospheric Pressure. *Geneva, I*, 1–32.
- YANG, Y. shan, GUO, X. xia, LIU, H. fang, LIU, G. zhou, LIU, W. mao, MING, B., XIE, R. zhi, WANG, K. ru, HOU, P., & LI, S. kun. (2021). The effect of solar radiation change on the maize yield gap from the perspectives of dry matter accumulation and distribution. *Journal of Integrative Agriculture*, 20(2), 482–493. [https://doi.org/10.1016/S2095-3119\(20\)63581-X](https://doi.org/10.1016/S2095-3119(20)63581-X)
- Zhao, B., Liou, K. N., Gu, Y., He, C., Lee, W. L., Chang, X., Li, Q. B., Wang, S. X., Sciences, O., Angeles, L., Tseng, H. R., Leung, L. R., Hao, J. M., & Control, P. (2016). Impact of

buildings on surface solar radiation over urban Beijing. *Atmospheric Chemistry and Physics Discussions*, 0(January), 1–22. <https://doi.org/10.5194/acp-2016-3>



## List of abbreviations and symbols

% = Percentage

° = Degree

°C = Celsius

Cm = centimeters

CV = Coefficient of variation

E= East

ENE = East-northeast

ESE = East-southeast

hPa = hectopascals

KJ/m<sup>2</sup>/day = kilojoule per square metre and per day

mm Hg = millimeters of mercury

mm/day = millimeter per day

N = North

N/m<sup>2</sup> = Newton per square meter

NE = Northeast

NNE = North-northeast

NNW = North-northwest

NW = Northwest

P = Precipitation

RH = Relative humidity

S = South

SE = Southeast

SSE = South-southeast

SSW = South-southwest

Stdev = Standard deviation

SW = Southwest

T = temperature

W = West

WMO = World Meteorological Organization

WNW = West-northwest

WSW = West-southwest

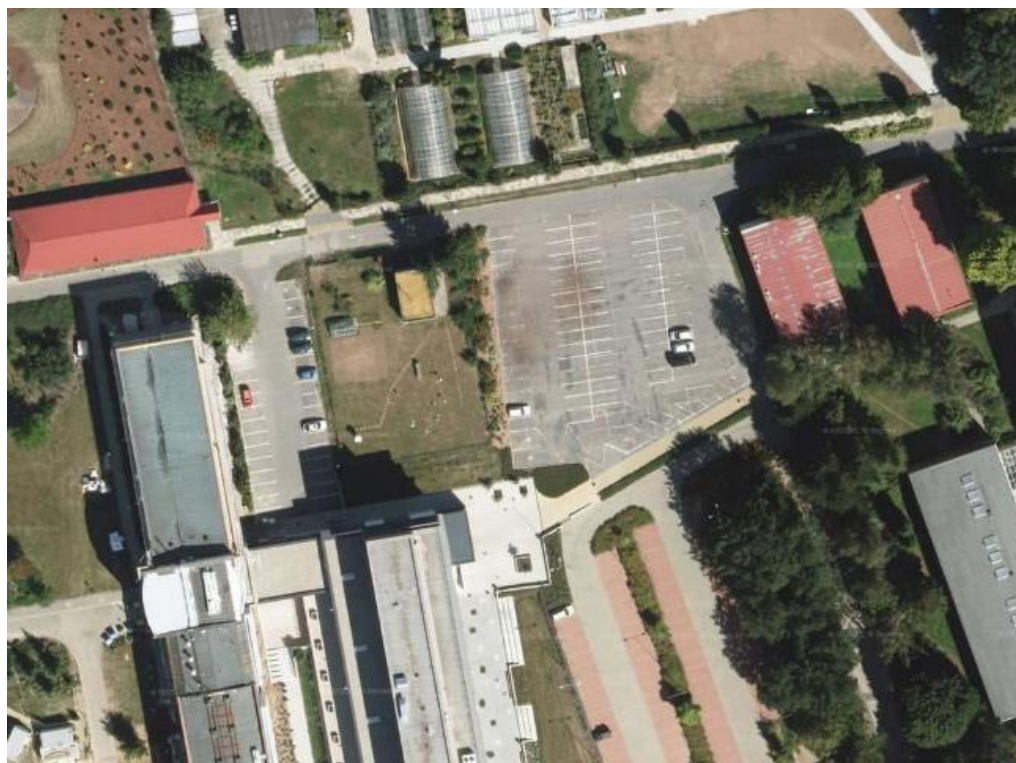
## **Appendices**

Appendix 1 Progress in built-up area surrounding the CZU meteorological station from 2012, 2015, 2018 and 2020

Appendix 2 Progress in built-up area surrounding the DWR meteorological station from 2012, 2015, 2018 and 2020

Appendix 3 Website climate record of CZU

Appendix 1 Progress in built-up area surrounding the CZU meteorological station from 2012, 2015, 2018 and 2020 (source: <http://www.mapy.cz>)



2012



2015





2018



2020



Appendix 2 Progress in built-up area surrounding the DWR meteorological station from 2012, 2015, 2018 and 2020 (source: <http://www.mapy.cz>)



2012



2015





2018




2020


# Appendix 3 website climate record of CZU (<http://meteostanice.agrobiologie.cz/>)

← → ↻ Not secure | meteostanice.agrobiologie.cz

Apps photosynthesis pro...



Meteostation of the Czech University of Agriculture Prague  
Faculty of Agronomy – department of Agroecology and Biometeorology

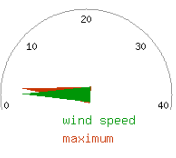
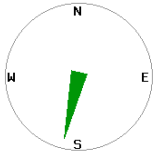
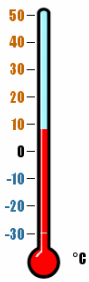


- Home
- About the site
- Data export
- How to read data
- Technical details
- Twb Calculator

### Last values

Saturday, 24. April 2021

Air temperature  Wind speed  maximum



Precipitation from last 7:00:

#### 15 (10) min values

- Air temperature
- Air humidity
- Air pressure
- Global solar radiation
- Wind speed
- Wind direction

#### Daily or 1 hour values

- Avg daily temp.
- Avg daily air humidity
- Temperature extremes
- Air pressure
- Wind speed & direction
- Wind maximum
- Precipitation
- Daily totals of precipitation
- Global solar rad /dav